



# **Linnæus University**

School of Computer Science, Physics and Mathematics

Degree Project

## **Design and simulation of beam steering for 1D and 2D phased antenna arrays using ADS**

**Supervisor: Prof. Sven-Erik Sandström**

**Department of Computer Science, Physics and Mathematics**

**Submitted for the degree of Master in Electrical Engineering**

**Specialization in Signal Processing and Wave Propagation**



**Authors: Muhammad Zeeshan Afridi, Daniyal Razi and Muhammad Umer**

**Date: 2012-06-18**

**Subject: Master Thesis**

**Level: Second**

**Course code: 5ED06E**

## **Acknowledgement**

We would like to express our sincere gratitude to our supervisor Dr. Sven-Erik Sandström for his continuous support, invaluable assistance and guidance during the entire period and in making this work possible. Deepest gratitude is also due to the Department of Computer Science, Physics and Mathematics, Linnaeus University, for providing the best educational facilities. We would also like to thank our seniors, fellow friends and siblings for their support and encouragement.

Last but not least, we would also wish to express our love and gratitude to our beloved families; for their support and understanding throughout our lives.

## **Abstract**

Phased arrays eliminate the problems of mechanical steering by using fast and reliable electronic components for steering the main beam. Modeling and simulation of beam steering for 1D and 2D arrays is the aspect that is considered in this thesis. A 1D array with 4 elements and a 2D array with 16 elements are studied in the X-band (8-12 GHz). The RF front-end of a phased array radar is modeled by means of ADS Momentum (Advanced design system).

**Keywords:** Phased array, Patch antenna, RF front-end, Beam steering, ADS Momentum.

# Table of Contents

Chapter one: Introduction	6
1. Introduction	9
1.1. Background	9
1.2. Thesis motivation	9
1.3. Thesis objective	9
1.4. Thesis overview	10
Chapter two: Literature review	11
2.1. Antennas	11
2.2. Antenna types	12
2.3. The microstrip patch antenna	12
2.4. Shapes of patch antennas	13
2.4.1. Substrate for the patch antennas	14
2.5. Antenna arrays	14
2.6. The Phased array	14
2.6.1. Principle of the phased array	15
2.6.2. The passive phased array	16
2.6.3. The active phased array	16
2.6.4. Array configuration	17
2.6.5. Array size	17
2.6.6. Active input impedance	17
2.6.7. Spacing between adjacent elements	18
2.6.8. Beam steering	18
2.7. Radar	20
2.7.1. The radar equation	20
2.7.2. Radar cross section	20
2.7.3. The TR module	21
2.7.4. Literature about the TR module	22
2.8. System modeling and specification	23
2.9. Target modeling	23
Chapter three: System design and modeling	24
3.1. Antenna design	24
3.1.1. The design process	24
3.1.2. Design specification	24
3.1.3. Design parameters	24
3.1.4. Mathematical model of the patch antenna	25
3.1.5. Designing of a rectangular patch antenna	27
3.1.6. The Antenna array	28
3.2. Complete system model	29

3.2.1.	The RF pulse transmitter	29
3.2.2.	The RF power divider network	29
3.2.3.	System level modeling of the TR module	30
3.3.	1D antenna array design	31
3.4.	2D antenna array design	32
3.5.	Radar front end modeling	34
3.5.1.	Signal analysis	35
Chapter four: Simulation results and analysis		37
4.1.	The single element side feed patch antenna	37
4.1.1.	Radiation pattern and gain	38
4.1.2.	3D radiation pattern	39
4.2.	Simulation of a 1D phased array antenna	40
4.2.1.	Radiation pattern and gain	40
4.2.2.	3D radiation pattern	41
4.3.	Simulation of a 2D phased array antenna	42
4.3.1.	Directivity and gain	43
4.3.2.	$S_{11}$ parameters	44
4.3.3.	Efficiency and radiated power	45
4.3.4.	3D Radiation pattern	46
4.4.	Simulation of beam steering of a linear array	47
4.5.	Simulation of beam steering of a 2D array	48
4.6.	The RF front end	49
Chapter five: Conclusion		51
5.1.	Conclusion	51
5.2.	Future work	51
References		52

## Table of Figures

Figure 2.1: Shapes of patch antennas.....	13
Figure 2.2: The phased array transmitter .....	15
Figure 2.3: Block diagram of a passive phased array .....	16
Figure 2.4: Block diagram of an active phased array .....	17
Figure 2.5: Beam steering .....	18
Figure 2.6: 2D antenna array arrangements.....	19
Figure 2.7: Block diagram of a typical TR module.....	21
Figure 2.8: Common phase shifter configuration of a TR module. ....	21
Figure 2.9: Seperate phase shifter configuration of a TR module. ....	22
Figure 3.1: Patch and Ground plane. ....	22
Figure 3.2: Top view of rectangular patch antenna.....	26
Figure 3.3: Series feed. ....	26
Figure 3.4: Corporate feed.....	29
Figure 3.5: An antenna array using corporate feed layout designed in ADS Momentum. ....	29
Figure 3.6: The Wilkinson power divider network 1:16 schematic designed in ADS Momentum.....	30
Figure 3.7: Radar TR module schematic designed in ADS Momentum.....	31
Figure 3.8: 1D Antenna array schematic designed in ADS Momentum.....	32
Figure 3.9: 1D Antenna array layout designed in ADS Momentum. ....	33
Figure 3.10: 2D Antenna array designed in ADS Momentum.....	33
Figure 3.11: 2D Square patch antenna array designed in ADS Momentum. ....	34
Figure 3.12: System level model of an active phased array radar system.....	34
Figure 3.13: The Switching signal.....	35
Figure 4.1: Single element side-feed patch antenna designed .....	37
Figure 4.2: $S_{11}$ -parameter of single side-feed patch antenna in .....	38
Figure 4.3: Radiation pattern of single side-feed patch antenna .....	38
Figure 4.4: Gain of the single side-feed patch antenna .....	39
Figure 4.5: A 3D graph of the far field radiation of a single square patch Antenna .....	39
Figure 4.6: 1D Phased array patch antenna designed .....	40
Figure 4.7: Radiation pattern of a 1D phased array antenna .....	40
Figure 4.8: Gain of a 1D phased array antenna .....	41
Figure 4.9: Excitation of 1D phased array antenna obtained with ADS .....	41
Figure 4.10: Top view of a 1D phased array antenna .....	42
Figure 4.11: Three dimensional view of a 2D phased array patch antenna .....	42
Figure 4.12: Gain and directivity of a 2D phased array patch antenna in.....	43
Figure 4.13: The magnitude vs frequency graph of $S_{11}$ .....	43
Figure 4.14: The corresponding phase of $S_{11}$ .....	44
Figure 4.15: $S_{11}$ plotted on a smith chart for frequency band 8-12 GHz. ....	44
Figure 4.16: Efficiency of the 2D phased array patch antenna .....	45
Figure 4.17: Radiated power of the 2D phased array patch antenna .....	45
Figure 4.18: 3D Directivity pattern of the 2D phased array antenna .....	46
Figure 4.19: Functional block diagram of beam steering.....	46
Figure 4.20: Simulation of a Linear array beam steering in. ....	47
Figure 4.21: Simulation of beam steering of a 2D array. ....	48

Figure 4.22: Transmitted pulse, time domain. ....	48
Figure 4.23: The amplitude of the transmitted pulse in frequency domain .....	49
Figure 4.24: Reflected signal, time domain. ....	49
Figure 4.25: The amplitude of the reflected signal in frequency domain. ....	50

## List of Tables

Table 3.1: Parameters of the desired antenna.....	27
Table 3.1: Dimensions of the rectangular patch.....	27
Table 3.2: Dimensions of the quarter wave transformer.....	27
Table 3.3: Dimensions of the feed line.....	27
Table 4.1: Relative phase of the elements in degrees.....	48



# Chapter one: Introduction

## 1. Introduction

This chapter gives a brief introduction to the thesis along with the objectives and the motivation behind this thesis.

### 1.1. Background

Radar is an acronym for Radio Detection and Ranging. It refers to a device which uses a radio frequency signal for the detection and ranging of targets. The principle is to measure the time delay between the transmitted and received RF pulse and through analysis determine the range and speed of the target. The radar antenna is used to focus energy in the direction of interest. A key issue in the design of an antenna is its side lobes. Side lobes are extremely harmful to the radar system as it is difficult to separate main lobe from side lobe reflections. Another disadvantage with the side lobes is that they make it easy for a jamming system to detect the radar. In order to solve the side lobe problem, various complex antenna designs were proposed. Via the intermediate step of fixed arrays this led to the present phased arrays.

Phased arrays are based on the principle that a consistent phase shift (time delay) in the signals that are feed to the antenna elements can be used to steer the main lobe in the desired direction. Phased array radars did not become airborne until the late eighties and was mainly used for ground based applications because of the substantial volume of the hardware involved. The obvious benefits of the phased array and continuous research has made it possible to develop phased arrays based on monolithic microwave integrated circuits (MMIC's) [1].

### 1.2. Thesis motivation

Considering the importance and the numerous applications of phased array technology, in defence, medical and other commercial applications like mobile and satellite communication, this thesis focuses on the system level modelling and simulation of the front-end of the phased array radar. The phased array has numerous applications as it is energy-efficient and agile as compared to traditional technologies. This technology is mostly used for defence purposes but considering its potential, one can safely assume that it will be adopted in many other applications in the future.

### 1.3. Thesis objective

The objective is to design and simulate antenna elements at system level with the emphasis on the front end of the radar without going into the details of signal processing. It is desired to develop a model of the phased array radar that can verify basic concepts of the radar front end. Specifically, one wants to simulate antenna elements at the targeted frequency by means of advanced design software. Arrays in 1D (4x1) and 2D (4x4) are also simulated.

## **1.4. Thesis overview**

**Chapter 1:** Brief introduction to phased array technology.

**Chapter 2:** It gives a summary of the literature reviewed during the research work. The process of designing a patch antenna, an antenna array and beam steering is described. A brief overview of the TR module, the RF front end and the complete system model is given.

**Chapter 3:** This chapter deals with the actual modeling of the system. Designing the patch antennas at the targeted frequency (x-band), modeling of the TR module and the RF front end of the phased array radar.

**Chapter 4:** This chapter presents the simulation results, which includes results from the designed antennas, simulation of beam steering both for the 1-D (1x4) and 2-D (4x4) array and the results for the RF front end using a pulsed RF signal.

**Chapter 5:** This chapter concludes and identifies directions for an extension of this work.

## Chapter two: Literature review

### 2.1. Antennas

An antenna is a device which transmits and receives electromagnetic energy. The energy, in the form of waves with combined electric and magnetic fields is propagating in space. In order to have a successful communication, two antennas, an antenna to transmit and an antenna to receive, are needed. At the transmission side, the electric energy (current and voltage) is converted into electromagnetic energy and at the receiver side the electromagnetic energy is converted back into electric energy. In order to transmit efficiently, the physical size of the antenna must be at least one-tenth of the wavelength. It is the operating frequency rather than the bandwidth that determines the size even though they are linked [2].

Antennas fall into two categories based on the radiation pattern: omnidirectional and directional. In principle the omnidirectional antenna exists only in textbooks since the dipole is the simplest electromagnetic source. A directional antenna focuses energy in a certain direction. An antenna system provides the following functionality.

- Concentrates energy in the direction of the target.
- Collects the echoes reflected by the target.
- Estimates the angle of arrival (azimuth and elevation) from the received echo signal.
- Determines the range (distance) to the target.
- Acts as a spatial filter and resolves its scan area into angles. It receives signal only in the direction of the main lobe and rejects signals coming from the other directions [3].

Important antenna parameters are gain, directivity, input reflection coefficient. The directivity is an important parameter of an antenna and for radar applications the antenna needs to be very directive. The efficiency of an antenna is also a prominent figure-of-merit for the overall effectiveness of the system. Antennas have gone through great advancements due to the continuous research efforts on bandwidth, efficiency, gain and size. Many compact and light weight antennas are being developed for airborne applications.

In a phased array radar, it is not the single element's radiation pattern that is essential but rather the radiation pattern of the whole array. The directivity of an array depends on the number of elements as well as the arrangement of the elements [4].

## **2.2. Antenna types**

Parabolic reflectors are mostly used in mechanical steered antenna systems. The reflector dish reflects the field from a source at the focal point. A point source generates EM waves, which are then directed by the reflector. Similarly, during reception, the reflector collects and directs energy to its focal point. Parabolic reflectors can have large apertures, which allows the system to receive more energy. Similarly, it can concentrate energy in a very narrow beam during transmission and thus have large gain.

The broadside array is another type of antenna that is used in many radar systems. It has a number of radiating elements, placed a half wave length apart, with a flat reflector behind the elements. The radiation is essentially perpendicular to the array and the reflector directs energy in the desired direction.

Microstrip patch antennas are also used for radar applications. High directivities can be achieved since they are easy to fabricate. The number of patches in an antennas in an array can reach one thousand.

## **2.3. The microstrip patch antenna**

The basic parameters of a microstrip antenna are covered in this part of the chapter. Step by step, the design process of the microstrip antenna is also explained.

In the quest for lightweight and compact antennas the microstrip antenna was a significant development. Microstrip patch antennas are, due to their size, weight, ease of manufacture and installation, very useful in medical, industrial and military applications. Unlike other types of antennas, prototypes can easily be manufactured.

Patch antennas have certain disadvantages; they have low power handling capability, a very wide beam and their bandwidth is also very narrow. In severe jamming situations, wideband antennas are very useful to reduce the jamming effect on radar and for this reason the antenna needs wideband impedance matching. Patch antennas are also developed for phased array applications. Space based radar systems have additional requirements on mechanical and thermal properties. 2D antenna arrays can be further divided into sub arrays for handling purposes. To achieve the required bandwidth, the dual stacked patch technique was used in combination with the probe feed technique. It was found that the beam steering in the azimuth plane with horizontal polarization was limited to 30 degrees with a return loss of 10 dB. When the scanning area was increased to 45 degrees the return loss dropped to 7 dB [2, 4].

## 2.4. Shapes of patch antennas

Some of the very common shapes of the patch antennas are shown in Figure 2.1.

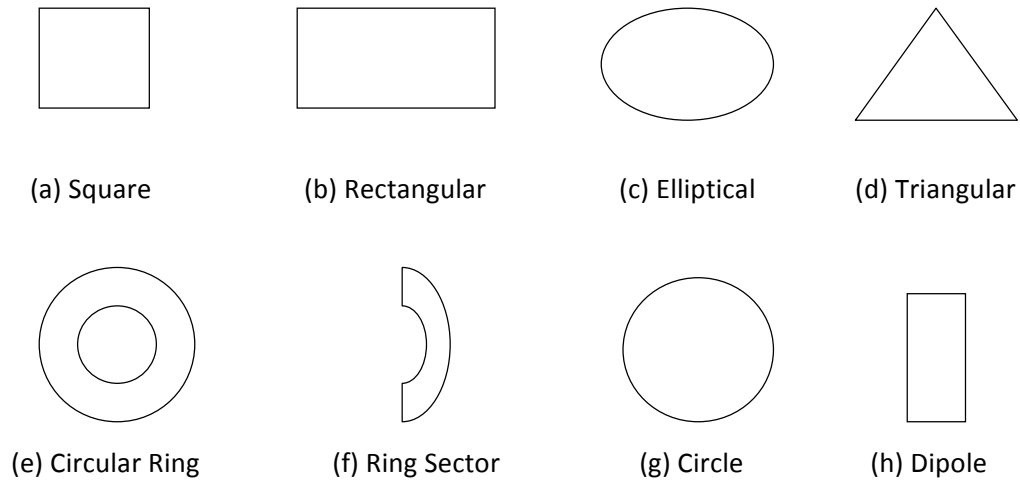


Figure 2.1: Shapes of patch antennas.

The most common shapes are circular and rectangular patches. These two shapes are favoured because of their mathematical models and radiation characteristic; hence they are easily described and therefore used in this work. Their equivalent mathematical models can be found in various forms in the literature [2]. Along with the shape, the type of substrate is essential for the patch.

### 2.4.1. Substrate for the patch antennas

An important constituent in the design of a patch antenna is the substrate. There are two common substrate materials available in the market, FR-4 and Roger duroid.

The FR-4 is a cheap substrate material, and it is also easily available in the market. The problem with this material when compared with the Rogers is that it has a very high loss tangent. Its loss tangent also changes with the frequency; higher frequency generally leads to more losses in FR-4. This property of the FR-4 explains some of the differences between the measured and the simulated results. Therefore, FR-4 is not preferred when accuracy is essential. Roger duroid, on the other hand, has all the benefits which FR-4 lacks, but it is a very expensive material. In this thesis FR-4 is used due to its availability and price [5].

## 2.5. Antenna arrays

The antenna array is based on the principle that when antenna elements are arranged in an array, the directivity of the radiation pattern increases. Initially, antenna arrays were used to increase the directivity and gain of the resulting beam of energy, but it was later found that beam steering can also be managed by a delay at each antenna element. The number of antenna elements and their arrangement are important for the directivity and the beam steering capability of the radar. As a general rule, the directivity of the array increases with the number of elements since the total aperture gets larger.

Depending on the scan area, antennas can be arranged on 2D surfaces such as spheres and cylinders. These arrays have their own issues like impedance matching with a varying scan angle and mutual coupling between the antenna elements. Ring arrays have a less directed radiation pattern and large grating lobes [4].

## 2.6. The Phased array

The phased array has the capability of varying the phase or introducing time delay at each antenna element in order to steer the main lobe. Despite all the efforts and development in this area, the phased array is still a very expensive technology. Researchers are making efforts to reduce the price by using cost effective components in order to make it viable commercially. Ultrasonic phased arrays are used to detect faults in mechanical structures without deforming the material [6].

A phased array has certain limitations; one of its shortcomings is the practical scan angle. Typically, the scan angle of the phased array is between 45 and 60 degrees. There are two factors responsible for this limitation; one is the effective length of the antenna. The effective length of the array decreases with the increasing scan angle and it becomes zero at an angle of 90° according to Eq. (2.6.1).

$$L' = L \cos(\theta) \quad (2.6.1)$$

$L'$  is the effective length of the array,  $L$  is the actual length and  $\theta$  is the scan angle.

### 2.6.1. Principle of the phased array

A phased array is composed of a number of radiating elements, each with a phase shifter. Deflection of the main beam can be achieved by introducing a phase difference between the elements. The electronic steering capability offers control of the directivity and gain. This eliminates the need for mechanical rotation [7].

In the phased array transmitter/receiver configuration the beam is focused to the direction of interest. Possible interference from any other direction can be avoided by creating a null in that direction, thus providing a capability for avoiding interference.

Transmission and reception are linked by the reciprocity theorem. Figure 2.2 shows  $m$  transmitters having a delay element in each line. When an input signal  $S(t)$  is fed to each element, the signal is delayed by the multiple of  $\tau$  and the resulting signal is given by Eq. (2.6.2),

$$S_r = \sum_{k=0}^{m-1} S(t - k\tau - (n-1-k) \frac{d \sin \theta}{c}) \quad (2.6.2)$$

Therefore, signals from the elements add coherently in a desired direction  $\theta = \sin^{-1} \frac{c\tau}{d}$ , while in other directions they essentially cancel.  $d$  is the spacing between the elements and  $c$  is the speed of light. It is the coherent addition that increases the radiated power in the desired direction.

At reception, the signal arrives at different points in time to the antenna elements and the time difference is then used to find the direction of arrival. The direction of arrival estimation is a highly active research field both for radar and telecommunication.

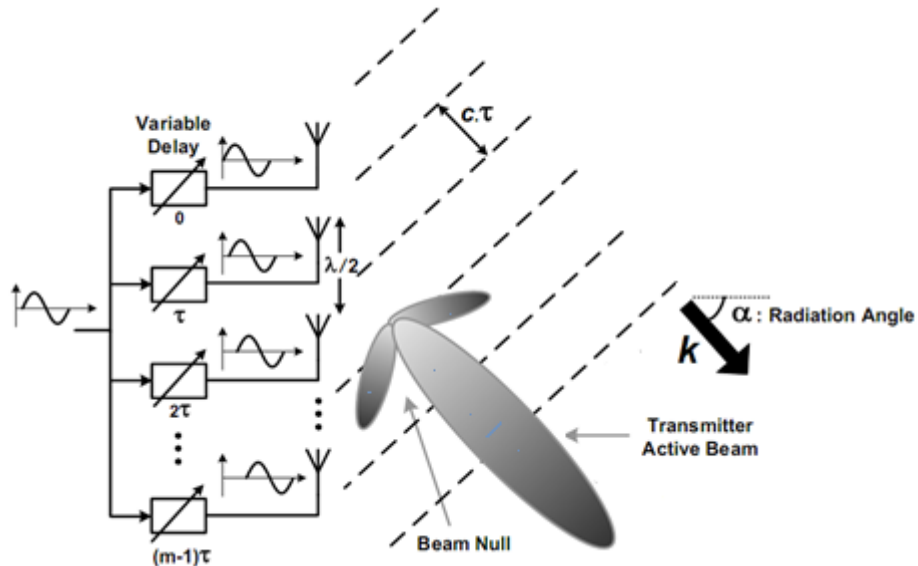


Figure 2.2: The phased array transmitter.

### 2.6.2. The passive phased array

An array with only one transmitter and receiver is referred to as passive. The beam steering is done with phase shifters at the antenna elements as shown in Figure 2.3.

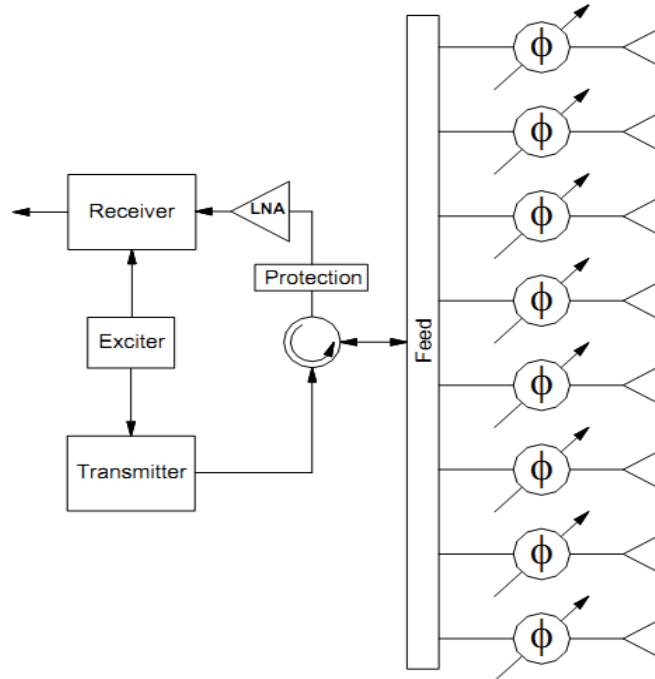


Figure 2.3: Block diagram of a passive phased array.

The passive array has a high power amplifier (PA) in the transmit path and a low noise amplifier (LNA) in the receive path. This design is less reliable and requires high power handling capability in the transmit path. These shortcomings are eliminated in the active phased array [8].

### 2.6.3. The active phased array

The active array has a T/R module for each antenna element. The T/R module consists of a transmitter, receiver, phase shifter, TR switch and duplexer.

The system will not shut down, if one of the TR module stops working. Since the phase shifter precedes the transmitter the power is low. Another main advantage of the active phased array is the multiple beam handling capability. Since the elements are fed independently one may have multiple beams operating at multiple frequencies. The receiver is placed close to the antenna to reduce losses.



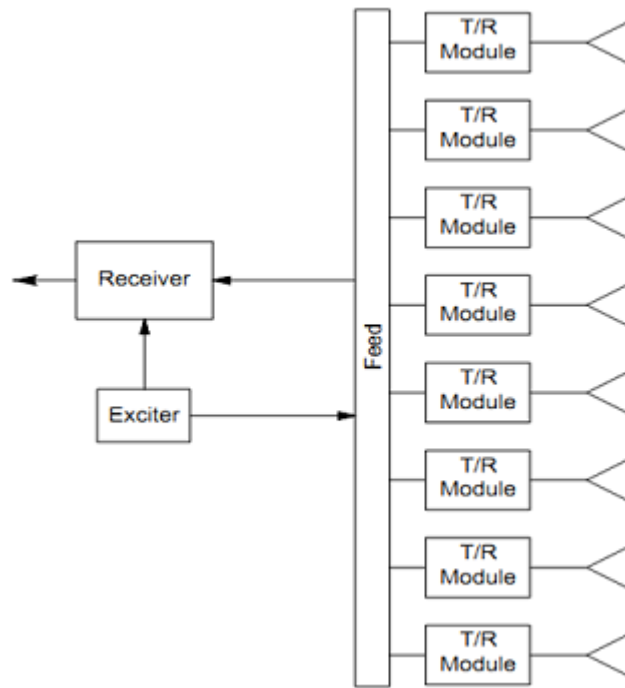


Figure 2.4: Block diagram of an active phased array.

#### 2.6.4. Array configuration

The array configuration is the geometrical arrangement of elements in an array. The simplest configuration has elements in a rectangular or quadratic planar grid. Another configuration described in the literature is the circular array. The structure looks like a big circular antenna. This type of antenna can be found in the front of jet planes.

#### 2.6.5. Array size

The array size determines the directivity, since directivity increases with the number of elements. The number of elements in an array may vary from a few to a thousand depending on the application. In defence radars, the numbers of elements is extremely large [9].

#### 2.6.6. Active Input Impedance

The active input impedance is one of the factors that limit the usefulness of the phased arrays. It comes into action when the array is scanning at large angles and it is due to induction from other radiating elements. The voltage source that feeds an element is not the only source acting on the element. The surrounding elements couple to the first element and this effect becomes severe as the angle of the beam increases. The coupling depends on the spacing between the elements [9].

### 2.6.7. Spacing between adjacent elements

The antenna elements are typically half a wave length apart. An increase in the element spacing up to  $0.9 \lambda$  increases the directivity but it also increases the side lobe levels. The important parameters in array design are element spacing and the number of elements.

### 2.6.8. Beam steering

The electronic steering has many advantages over mechanical steering: agility, accuracy, flexibility. It can be used to track targets maneuvering at greater speeds due to the flexible electronic control of the main beam. Since there is no physical movement of the structure, the system is less prone to wear and tear and is more durable than the mechanical systems.

The principle of beam steering can be easily understood with the help of Figure 2.5. Steering can be achieved by means of a phase difference between radiating elements. In Figure 2.5, four elements are arranged in linear array, with the spacing  $d$  between adjacent elements [9]. With this arrangement, the  $N$ th element has a delay of  $(N-1)(\Phi)$ .

$$x = d \sin \theta_s \quad (2.6.3)$$

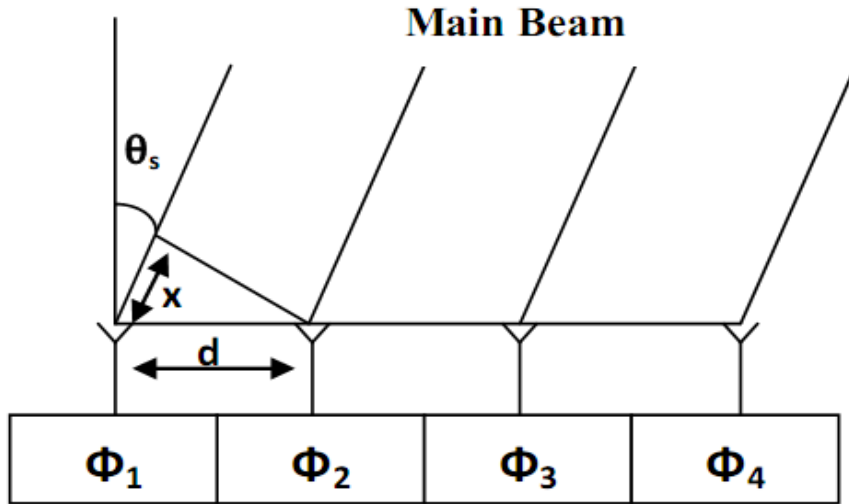


Figure 2.5: Beam steering.

The phase difference  $\Phi$  corresponds to a path difference  $x$  between the two adjacent beams. The ratio of the path difference  $x$  to the wavelength  $\lambda$  should be equal to the ratio of the phase difference  $\Phi$  to  $2\pi$  ( $360^\circ$ ), because  $2\pi$  is the angle corresponding to one wavelength.

$$\frac{2\pi}{\Phi} = \frac{\lambda}{x} \quad (2.6.2)$$

Using Eqs. (2.6.3) and (2.6.2) the angle  $\Phi$  is then given by,

$$\phi = \frac{2\pi d \sin \theta_s}{\lambda} \quad (2.6.3)$$

where  $d$  is the element spacing and  $\theta_s$  is the desired angle of steering.

The complexity of beam steering increases if a 2D array is considered. In 2D, the beam can be steered in two directions. A 4x4 array is shown in Figure 2.6 .

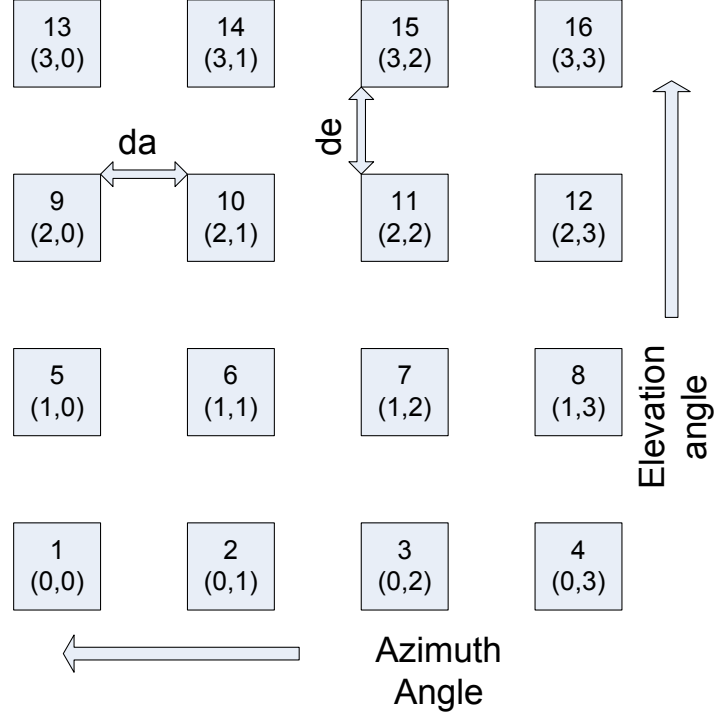


Figure 2.6: 2D antenna array arrangements.

The elements are arranged in a matrix of rows and columns as indicated by the numbers. The first element (0, 0) is used as a phase reference. The direction of the beam is specified in polar coordinates  $(\theta, \phi)$ .

The relative phase difference between the antenna elements in 1D and 2D arrays are given by Eq. (2.6.3) and (2.6.5), respectively.

$$\Delta\phi_{r,c} = k[r d_r \sin \phi + c d_c \sin \theta] \quad (2.6.5)$$

Here  $k = \frac{2\pi}{\lambda}$ , and  $r$  and  $c$  is the row and column number of the element, respectively.  $d_r$  is the distance between the elements in a row and  $d_c$  is the distance between the elements in a column. The azimuth angle to be steered is  $\phi$  and the elevation steering angle is  $\theta$ .

## 2.7. Radar

A radar has a transmitter that radiates electromagnetic waves toward a target. In the case of a monostatic radar the target reflects the waves back to the receiver. In the bistatic case the waves are received by a receiver that is not located at the transmitter. The strength of the reflections from the target depends on the size, shape and electrical conductivity of the target. The basic idea of radar dates back to the late 19th century, but the principal development of radar technology did not occur until World War II. Today, radar is used extensively in a number of civilian applications, e.g. air-traffic control, remote sensing of the environment, aircraft and ship navigation, space surveillance and planetary observation [3].

### 2.7.1. The radar equation

The radar equation relates the transmitted and received power to the range of the radar. The received power  $P_r$  is given by,

$$P_r = \frac{P_t A_e G \sigma}{(4\pi)^2 R^4} \quad (2.7.1)$$

$P_t$  is the transmitted power,  $G$  is the gain,  $A_e$  is the effective aperture of the receiving antenna, given by the physical area and the aperture efficiency,  $\sigma$  denotes the radar cross section and differs from the physical area of the target.

Equation (2.7.1) can be used to estimate the maximum range of a radar. Every system has a certain sensitivity floor below which the system cannot differentiate the signal and the noise. Since the signal level decreases with range, there is limit where the receiver can no longer detect the target. The maximum range of a radar is given by,

$$R_{max} = \left[ \frac{P_t A_e G \sigma}{(4\pi)^2 P_r} \right]^{\frac{1}{4}} \quad (2.7.2)$$

This is the fundamental radar equation and gives the maximum range in terms of the parameters of the radar and the target.

### 2.7.2. Radar cross section

The radar cross section is denoted by  $\sigma$  and describes the scattering properties of the target. It represents the physical size of the target as seen by the radar and has the dimensions of square meters. The RCS area is a measure of a target's ability to reflect radar signals in the direction of the receiving antenna [2]. In general, the RCS is a function of the polarization of the incident wave, the angle of incidence, the angle of observation, the geometry of the target, the electrical properties of the target and the frequency of operation [10].

### 2.7.3. The TR module

The TR module is an integral part of the phased array radar. A typical configuration is shown in Figure 2.7.

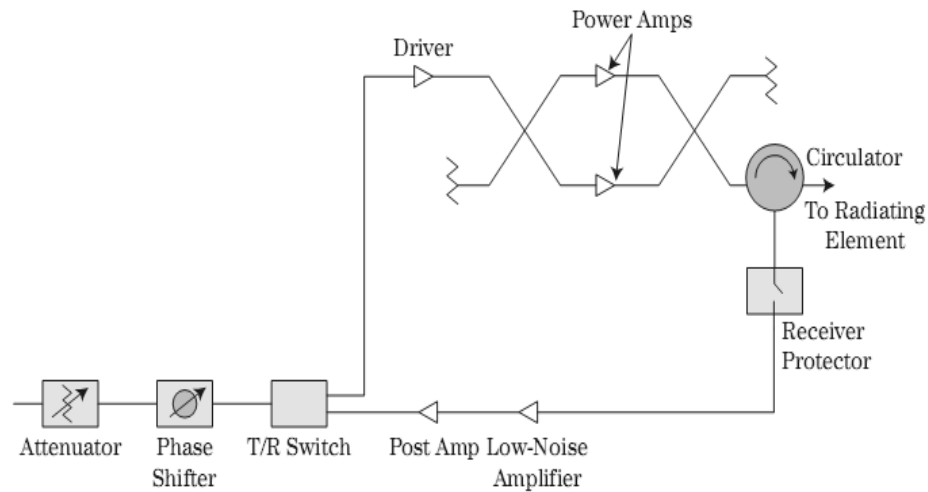


Figure 2.7: Block diagram of a typical TR module.

The essential components are:

**Attenuator:** The attenuator in a TR module adjusts the gain of the system to minimize the side lobes as well as to steer the nulls in the direction of interfering sources.

**Phase Shifter:** The phase shifter provides the required phase shift to steer the antenna beam.

**TR Switch:** The transmit/receive or TR switch controls the operation of the module. In most cases, it is a single pole double throw (SPDT) switch, that switches the system between the transmit and receive modes.

**Power Amplifier:** These gain blocks amplify the transmitted signal. The amplification depends upon the type of function and range of the radar.

**Circulator:** It is a passive device that connects the antenna to the transmit section and isolates the sensitive receive circuitry from the high transmit power.

**Limiter Circuitry:** This protection circuit is incorporated mainly to protect the low-noise amplifier from being saturated by high transmit power reflected backward due to the antenna mismatch. It also prevents the high power jamming signals from damaging the system.

**Low Noise and Post Amplifier:** The received signals are often weak and noisy. To extract meaningful information, the signal is amplified by a low-noise amplifier (LNA), to minimize the noise injected by the system [11].

#### 2.7.4. Literature about the TR module

There are different types of TR modules described in literature, in this case matters relating to phased array radars. The electrical design has two standard configurations, the common and the separated architecture [12]. In the common architecture, there is a single phase shifter that is being shared by the transmitter and receiver while the separate architecture has two phase shifters. The common and separate topologies are shown in Figures 2.8 and 2.9, respectively.

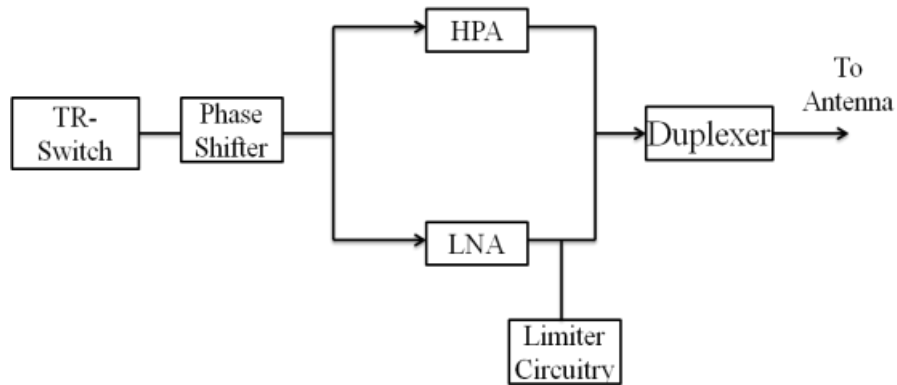


Figure 2.8: Common phase shifter configuration of a TR module.

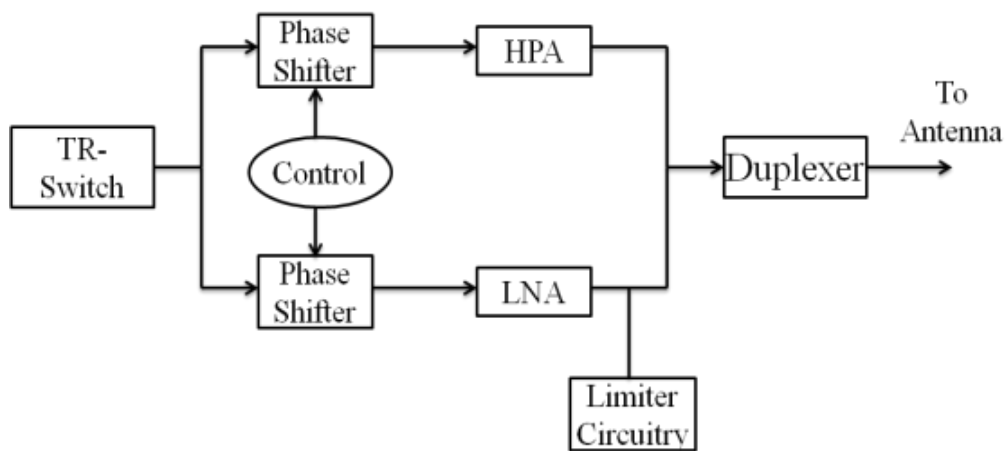


Figure 2.9: Separate phase shifter configuration of a TR module.

A hybrid mechanical/electrical systems can also be used. Azimuth scanning is performed by mechanical rotation while elevation scanning is done by means of electronic beam steering [12].

## 2.8. System modeling and specification

In any modeling, the first thing is to search for specifications of related systems in the literature. Literature was surveyed for specifications of operating phased array radars.

The quest for phased array radars started with a US navy venture in 1958. An extremely advanced system called typhon was developed in order to detect multiple targets. However, the project was later abandoned. A second attempt towards building a phased array was SPG-32 and SPG-33. Considering the failure of typhon, some of the system requirements were relaxed in SPG-32 & 33. The relevant technology was not mature at that time; transistors were not available on a mass scale and vacuum tubes had to be used. Despite all the challenges, the system was built and installed on war ships. The system failed, however, not due to the fundamental design but because of the subsystems and hence SPG-32 & 33 were abandoned in the late 70's.

After the failure of the first two projects, Spy-1 was the next attempt to build a phased array radar. Having learned from the first two failed attempts, designers mainly focused on the digital system controlling the beam. A prototype of the antenna was installed on a ship in 1974. Extensive testing of the system was carried out and the results were very impressive. Spy-1 operates in the S-band and utilizes four passive arrays with dimensions 3.65 m x 3.65 m. The beam width was 1.7 degrees [1, 13].

## 2.9. Target modeling

Accurate modeling of the target is closely related to the real time environment and is critical for the testing of the modeled system. In the case of radar, the signal strikes the target and returns back to the receiver where it is being analyzed. Theoretically, target reflections can be accurately characterized by the Maxwell equations, but the problem is that the solution of these equations is tractable only for simple target shapes. Therefore, radar designers look for a number of approximation techniques,

1. A scaled down version of the target which reduces the accuracy.
2. Use of a large number of antenna arrays in an anechoic chamber which illuminates the target from various directions [14].

The radar target modeling is a complex task and requires detailed information about the target geometry. Some targets can be visible within a very narrow angle while others are visible throughout. The objective of target modeling is to determine how much of the scattered field that comes back towards the receiver [10].

## Chapter three: System design and modeling

### 3.1. Antenna design

The antenna is an interface between the transmitter and free space. Various antenna designs were considered during the thesis work. Patch antennas were selected for further investigation because of advantages like compact size, light weight and ease of manufacturing. They have a number of medical, industrial and military applications. Unlike other type of antennas, they can easily be built for prototype purposes.

#### 3.1.1. The design process

The efficiency of an antenna is a prominent figure-of-merit. The antenna efficiency depends on the gain and the reflection coefficient (impedance matching). The port impedance is normally chosen to be 50  $\Omega$ . At high frequency, it is desirable to use low loss and high quality substrate materials such as Roger RT Duroid. However, for prototype purposes, FR-4 can be used since it is cheap and readily available. The design of a microstrip patch array is divided into four steps: defining specifications, design of a single patch, design of an array and simulation of an array [15]. Patches have many shapes: rectangular, circular and triangular [2].

#### 3.1.2. Design specification

The antenna used in radars needs to be very directive at the desired frequency. A low reflection coefficient is important in the design of the antenna feed. The four feeding techniques are: microstrip line, coaxial probe, aperture coupling and proximity coupling [2]. The microstrip line is used in this design due to its simplicity.

#### 3.1.3. Design parameters

The side and top view of the single patch along with the related parameters are shown in Figures 3.1 and 3.2, respectively. The substrate with relative permeability  $\epsilon_r$  is sandwiched between two conducting plates. The upper conducting plate is etched to produce the desired shape, while the lower conducting plate acts as a ground plane.

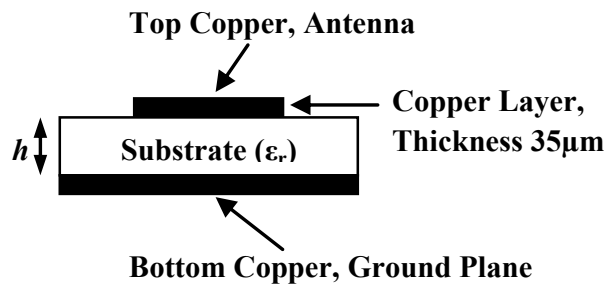


Figure 3.1: Patch and Ground plane.



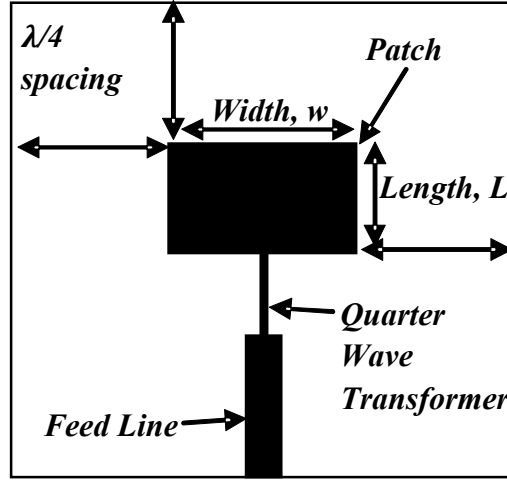


Figure 3.2: Top view of rectangular patch antenna.

The resonant frequency of the antenna depends upon the dimensions of the patch and the dielectric [15].

### 3.1.4. Mathematical model of the patch antenna

The cavity model or the transmission line model are conventionally used in the design of a microstrip patch. The simpler transmission line model is used here.

This model treats the patch antenna as an array of two radiating slots, separated by a low impedance transmission line of length  $L$  [2]. The transmission line method is used to find the parameters of the patch for desired performance [2, 16].

The first step is to find the width  $w$  of the patch at the desired frequency, using Eq. (3.1.1).

$$w = \frac{c}{2f_0 \sqrt{2(\epsilon_r + 1)}} \quad (3.1.1)$$

where  $\epsilon_r$  is the relative permittivity.  $c$  is the speed of light and  $f_0$  is the desired frequency. The length of the patch can be expressed in terms of the effective dielectric constant  $\epsilon_{eff}$ ,

$$L_{eff} = \frac{c}{2f_0 \sqrt{\epsilon_{eff}}} \quad (3.1.2)$$

To cater for the fringing effects, the actual length of the patch also includes a correction factor. The actual length is given by,

$$L = L_{eff} - 2\Delta L \quad (3.1.3)$$

The correction factor is given by,

$$\Delta L = 0.412h \frac{(\epsilon_{eff} + 0.300)(w/h + 0.264)}{(\epsilon_{eff} - 0.258)(w/h + 0.800)} \quad (3.1.4)$$

$h$  is the substrate height or thickness as shown in Figure 3.1.  $\epsilon_{eff}$  is given by,

$$\varepsilon_{eff} = \frac{\varepsilon_r + 1}{2} + \frac{\varepsilon_r - 1}{2} \frac{1}{\sqrt{1 + \frac{12h}{w}}} \quad (3.1.5)$$

The input impedance was transformed to 50  $\Omega$  for impedance matching. The impedance of the patch at the resonant frequency can be found using Eq. (3.1.6).

$$R_{in}(y = y_0) = \frac{1}{2(G_1 \pm G_{12})} \cos\left(\frac{\pi y_0}{L}\right) \quad (3.1.6)$$

$y_0$  is the distance from the radiating edge of the patch along the length  $L$ .  $G_1$  is the edge conductance or self-conductance of the radiating slot:

$$G_1 = \int_0^\pi \left[ \frac{\sin\left(\left(\frac{k_0 w}{2}\right) \cos \theta\right)}{\sqrt{120\pi} \cos \theta} \right]^2 \sin \theta^3 d\theta \quad (3.1.7)$$

$G_{12}$  is the mutual conductance between the two slots and is given by the following relation:

$$G_{12} = \int_0^\pi \left[ \frac{\sin\left(\left(\frac{k_0 w}{2}\right) \cos \theta\right)}{\sqrt{120\pi} \cos \theta} \right]^2 J_0(k_0 L \sin \theta) \sin \theta^3 d\theta \quad (3.1.8)$$

where  $k_0 = \frac{2\pi\sqrt{\varepsilon_{eff}}}{\lambda}$ ,  $\lambda$  is the wavelength and  $J_0$  is the zero order Bessel function. Both the array and the single element requires impedance matching [17, 18].

A quarter wave transformer is used for impedance matching at 50  $\Omega$ . The impedance  $R$  of the quarter wave transformer is given by  $R = \sqrt{Z_1 Z_2}$ . The transformer is designed with the microstrip line formulas above. The minimum distance between the radiating patch edge and the outer boundary should be greater than  $\lambda/4$  [19], as shown in Figure 3.2.

### 3.1.5. Design of a rectangular patch antenna

The antenna is designed and simulated at the desired frequency with ADS Momentum. The parameters are given in Table 3.1.

Table 3.1: Parameters of the desired antenna.

Shape	Rectangular patch
Frequency	2 GHz
Free space wavelength ( $\lambda_0$ )	0.15 m
Substrate	FR-4 ( $\epsilon_r=4.5$ )
Substrate height	0.0016 m

The dimensions of the antenna are determined with the formulas above and appear in Table 3.2.

Table 3.2: Dimensions of the rectangular patch.

Physical width of the patch (w)	0.049 m
Effective length of the patch (L)	0.0364 m
Correction factor	0.0014 m
Actual length (L)	0.035 m
Impedance at the patch edge	245.2 $\Omega$

The impedance of the patch at the edge is 245.2  $\Omega$  and must be transformed into 50  $\Omega$ . The impedance of the quarter wave transformer comes out to be 111.24  $\Omega$ . The dimensions of the quarter wave transformer were found with the txline calculator. The calculator requires basic information about the substrate along with the impedance and electrical length of the line. Using 90° electrical length and the 111.24  $\Omega$  impedance one obtains the dimensions in the table.

Table 3.3: Dimensions of the quarter wave transformer.

L (physical length)	0.021654 m
W (width of the transformer)	0.0004599 m

The input to the quarter wave transformer should be 50  $\Omega$ . The dimensions of the 50  $\Omega$  feed line are again found with the txline calculator. The impedance is 50  $\Omega$  whereas the electrical length is 180°. The dimensions of the feed line are given in Table 3.4.

Table 3.4: Dimensions of the feed line.

L (physical length of the feed line)	0.040585 m
W (width of the feed line)	0.2968

### 3.1.6. The antenna array

First, a 1D antenna is considered. The separation between the elements is one of the important parameters of an antenna array. The directivity increases when the elements are placed with the optimum separation of  $\lambda/2$  [21] and therefore this separation will be used. The next important issue is the feed to the antenna array and there are two types.

#### a. Series feed

In the series feed method, the antenna elements are connected in cascade. This type of feeding technique is used in fixed beam applications, as the signal of each element is dependent on the signal of the previous element. With this method, the main beam becomes more directed and focused.



Figure 3.3: Series feed.

#### b. Corporate feed

Corporate feed provides a  $1:2^n$  splitting. The splitting is done either by tapered line or by quarter wave transformer. Starting from the left side, there is a  $50\ \Omega$  feed line that splits into two  $100\ \Omega$  lines. The two  $100\ \Omega$  lines in parallel makes a perfect match for the  $50\ \Omega$  line. In the second step, a quarter wave transformer is used to transform the  $100\ \Omega$  line to  $50\ \Omega$  line. This process can be repeated again if further splitting is required.

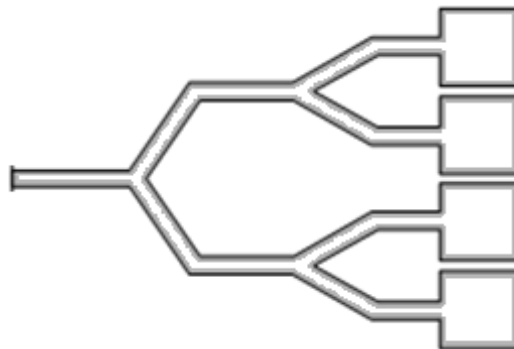


Figure 3.4: Corporate feed.

The antenna array was designed in ADS Momentum using corporate feed and an element spacing of about half a wavelength. The line impedances are shown in Figure 3.5; the dimensions of each line are found using the txline calculator.

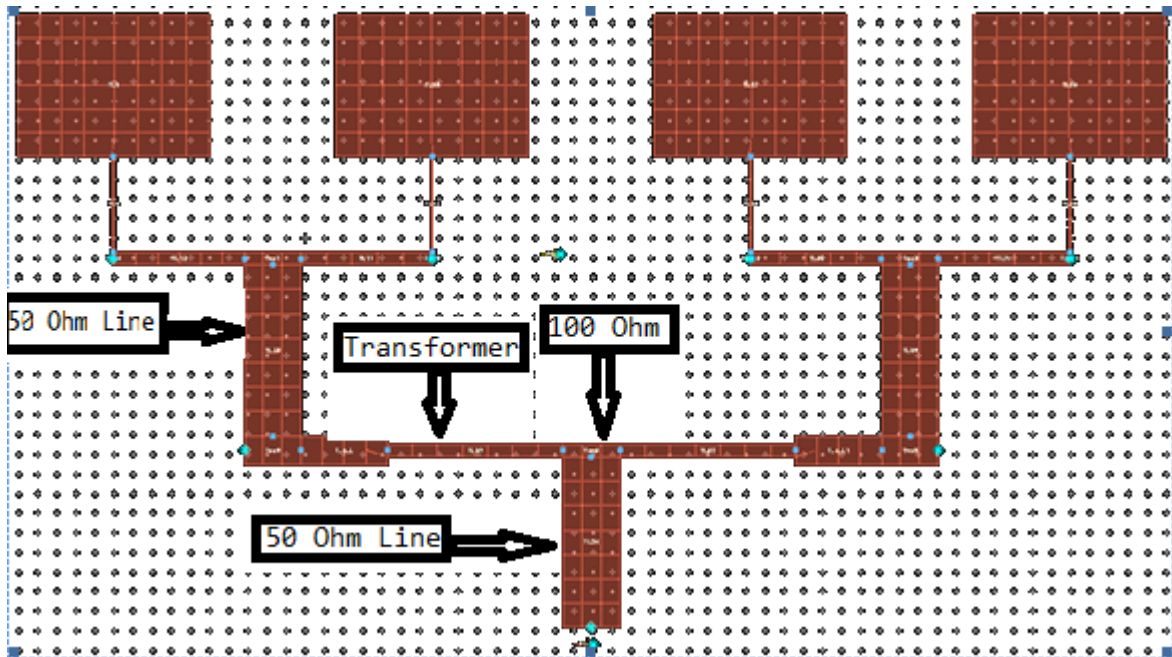


Figure 3.5: An antenna array using a corporate feed layout designed in ADS Momentum.

## 3.2. Complete system model

The system level modeling of the front-end of the phased array radar can be divided into modeling of the following subsections.

### 3.2.1. The RF pulse transmitter

The RF pulse generated at the transmitter has an ON and an OFF time. The time in which the pulse is transmitted is known as the ON time during which a signal of 9 GHz is sent, while the receive time is known as the OFF time. ADS schematics has a block for generating the required pulse.

### 3.2.2. The RF power divider network

Ideal power splitter blocks are used to build a network to divide the power with the ratio 1:16. These blocks provide 3 dB power splitting like the Wilkinson power divider. The frequency for the verification of the substrate parameters is 2 GHz.

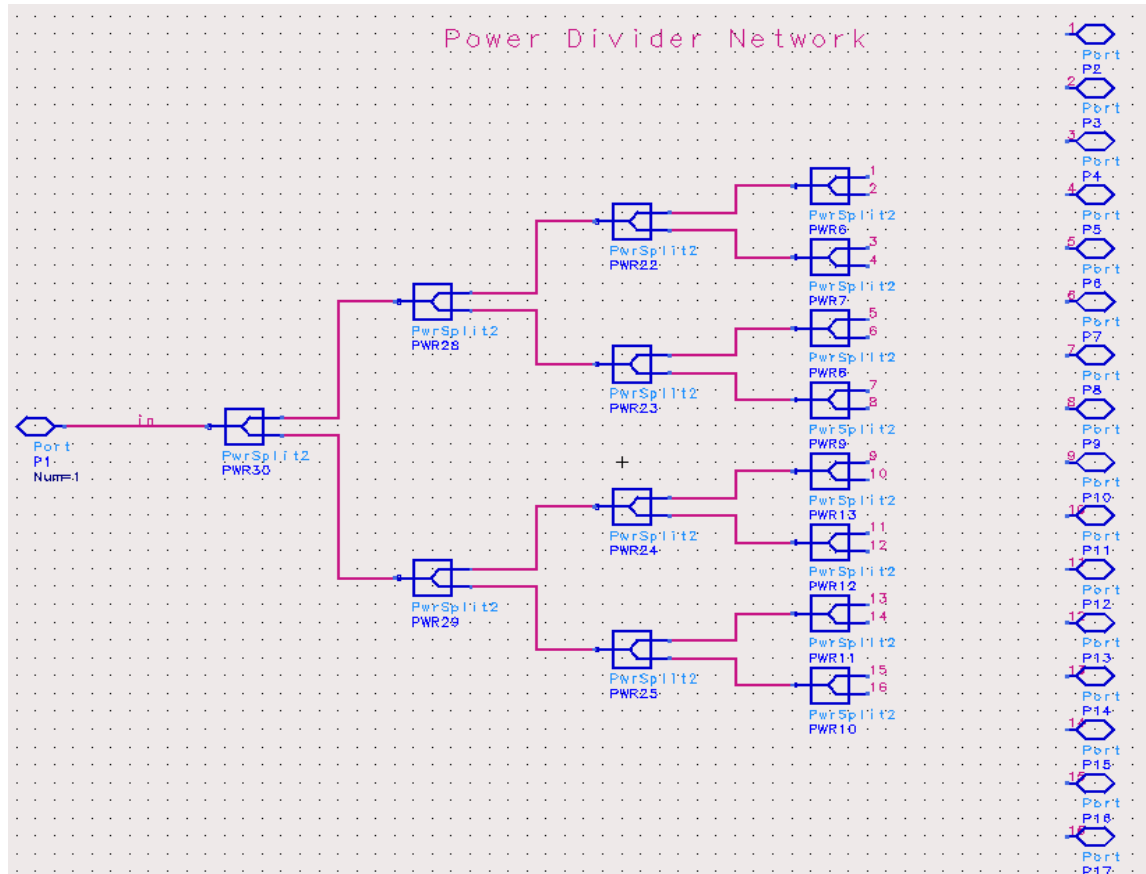


Figure 3.6: The Wilkinson power divider network 1:16 schematic designed in ADS Momentum.

### 3.2.3. System level modeling of the TR module

There are two basic configuration of TR modules, the common and the separate, where the separate has separate phase shifters for the transmitter and receiver. It is more costly but simplifies the handling of the phase and is therefore used here [8, 20].

The TR module is modeled by using built in blocks available in ADS. The TR switch and duplexer are modeled by a single-pole, double throw switch that is controlled by a clock signal. The lumped phase shifter, the high power amplifier and the low noise amplifiers are used for the modeling of the respective blocks. The TR module thus modeled is shown in Figure 3.7.

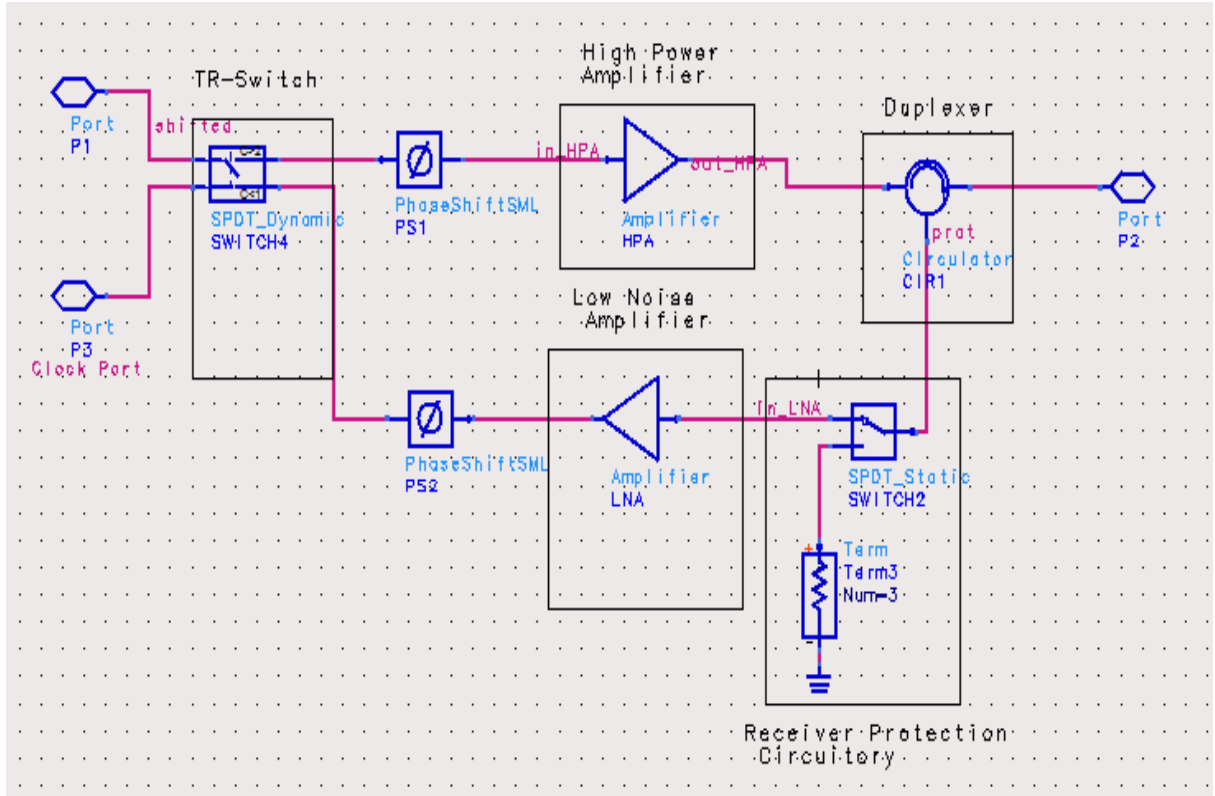


Figure 3.7: Radar TR module schematic designed in ADS Momentum.

There is one clock signal which is used to synchronize the whole system. This clock defines the ON and OFF period or differentiates between the transmit and receive mode. A high time of the clock selects the transmission mode while a low time defines the reception mode of the system.

The frequency of the system is 9 GHz. The high power and the low noise amplifier both have a gain of 20 dB. The module antenna has a gain of 8 dB and an array of sixteen elements has been used. The assumed target is at a distance of 10 m.

The simulation results are analyzed and discussed in chapter 4 of this thesis.

### 3.3. 1D antenna array design

After these preparations, the first objective is to achieve beam steering in a simulation by designing an array at the targeted frequency. A four element side feed array was modeled in ADS momentum using the typical half wavelength spacing between the elements.





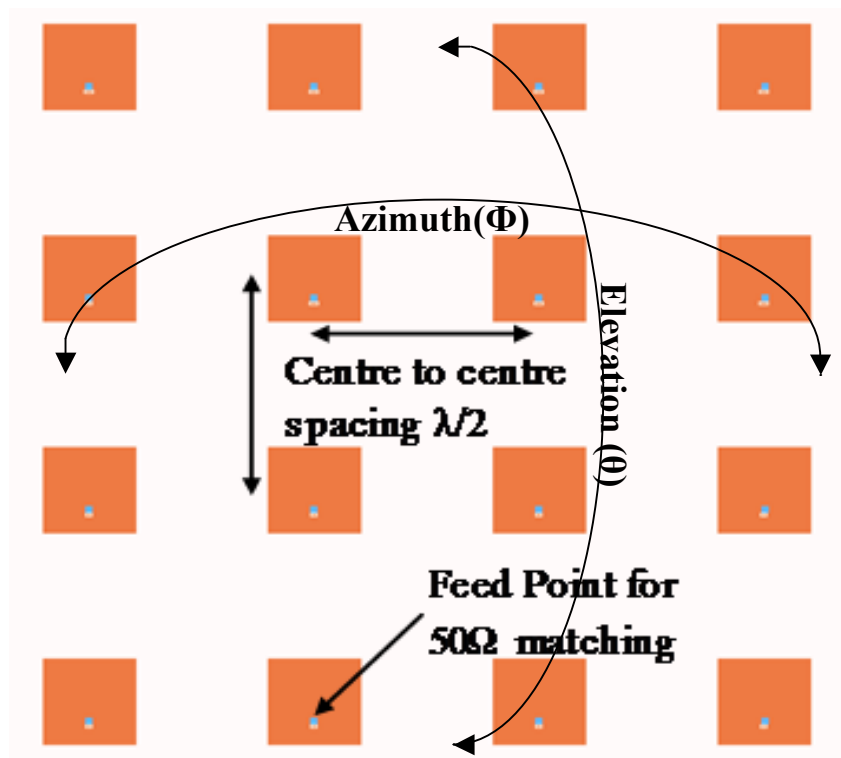


Figure 3.10: 2D antenna array designed in ADS Momentum.

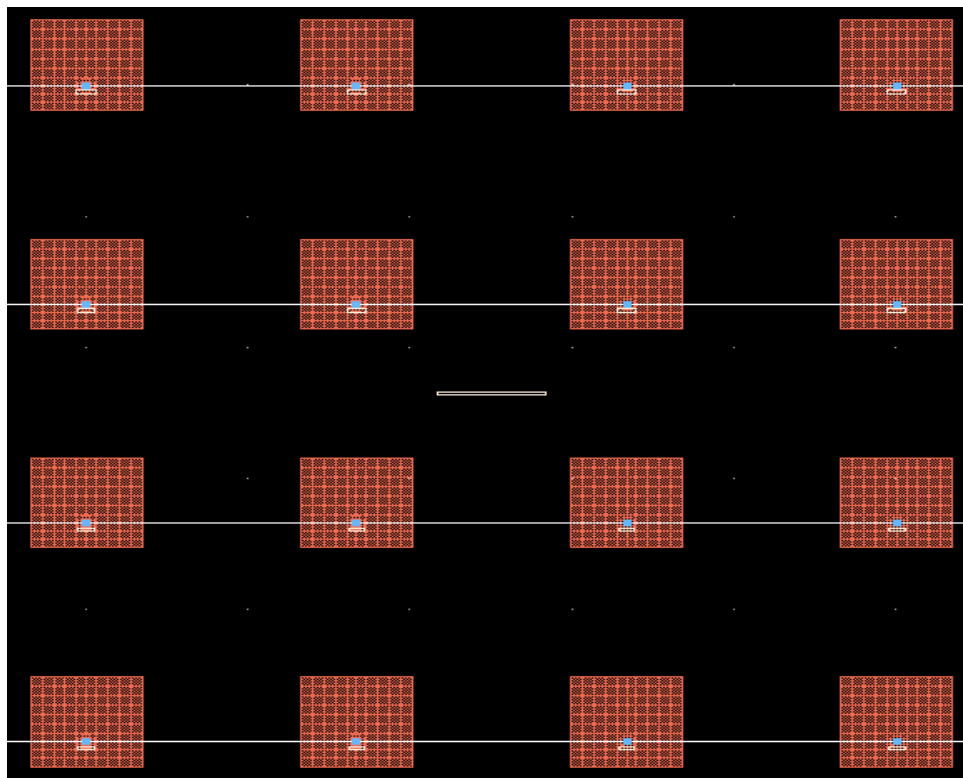


Figure 3.11: 2D square patch antenna array designed in ADS Momentum.

Considering the requirement to place the TR-modules before the antenna elements, the probe feed is preferred over the side feed in the array design.

The elementary beams of the antenna elements add up and form a single wave front. The signal then strikes the target and is reflected back towards the receiver. The formation of a single beam in free space is achieved with a network of passive RF combiners.

Measurement and simulation results are analysed and explained in chapter 4 of the thesis report.

### 3.5. Radar front end modeling

The system level simulation provides a framework to evaluate the performance of the designed components. It specifies the shortcomings of the designed modules and provides an opportunity to make further improvements. The block diagram of a typical active phased array radar on an abstract level is shown in Figure 3.12. The RF front end of the active phased array radar can be divided into three blocks: antenna array, array of TR modules and a receiver circuit. In addition, there is also a digital control circuit which defines the position of the antenna beam by providing the phase shift in each antenna element through phase shifters.

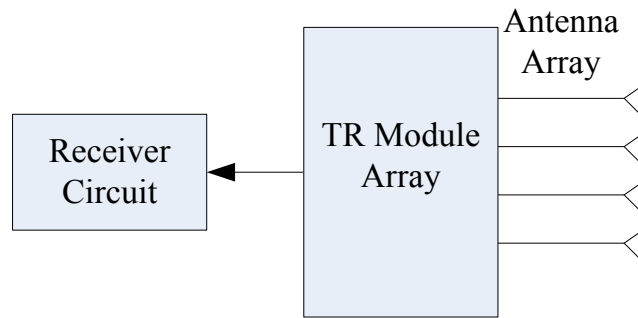


Figure 3.12: System level model of an active phased array radar system.

The beam must be very directive in radar applications, as it improves the efficiency and scan resolution by concentrating the energy in a narrow solid angle. In a phased array this objective is achieved by using many antenna elements [4].

### 3.5.1. Signal analysis

The continuous wave radars use two antennas, one for transmission and one for the reception of reflected energy, although there are systems that use a single antenna for both purposes. The CW radars are mostly used to measure the speed of the target. Most of the radars which use one antenna for both transmission and reception are pulsed radars; they are capable of measuring the speed as well as the distance of the target. The range is measured using the time delay of the pulse while speed is measured using the Doppler shift, i.e. the change in frequency of the RF pulse. Signal analysis, both in time and frequency domain and during transmission and reception is explained below.

In a pulsed radar, the RF pulse is transmitted for a certain period of time (ON time) after which it has a reception period known as OFF time. This signal that switches the mode of the system is called the switching signal (SS). The pulse is repeated after a certain period of time known as the pulse repetition time (PRT), having a corresponding pulse repetition frequency (PRF). The signal that switches between transmit and receive mode is shown in Figure 3.13.

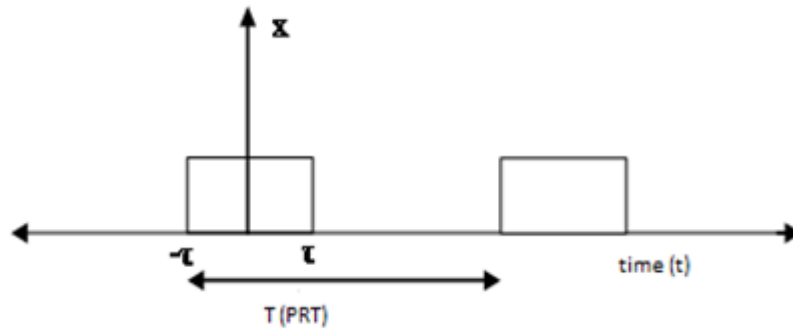


Figure 3.13: The switching signal.

The time domain representation is given by,

$$\begin{aligned} x(t) &= 1 & -\tau < t < \tau \\ &= 0 & \tau < t < T - \tau \end{aligned} \quad (3.5.1)$$

A large PRT increases the range of the radar since it corresponds to longer distances. The range also depends on the sensitivity of the receiver as the signal decays with distance. Hence, It becomes difficult for the receiver to differentiate between the reflected signal and the noise floor of the receiver. The PRT is therefore determined by the receiver's sensitivity and the maximum range (Run) that the radar can detect [3].

$$R_{un} = \frac{cT}{2} \quad (3.5.2)$$

c is the speed of light in free space and T is the pulse repetition time. The time domain representation of the RF signal transmitted during ON time is given by,

$$y(t) = \sin(2\pi f_r t) \quad (3.5.3)$$

The transmitted RF pulse that is being transmitted is the product of the RF signal ( $f_r$ ) and a switching signal SS. In the frequency domain the switching signal is transformed into a sinc function ( $T \gg \tau$ ) and the sinc function into two impulses at  $\pm f_r$ .

The Transmitted RF pulse in the frequency domain is given by the sinc functions,

$$X_1(f) = \text{sinc}(f - f_r) + \text{sinc}(f + f_r) \quad (3.5.4)$$

After passing through the TR module, the pulse is amplified in the power amplifier and the required phase is set by a phase shifter. With amplifier gain  $A_p$ , phase  $\Phi$  and antenna gain  $G_a$ , the first antenna element produces a signal,

$$X_1(f) = A_p G_a \text{sinc}(f - f_r) e^{-j\Phi_1} \quad (3.5.5)$$

and similarly from the second element one has,

$$X_2(f) = A_p G_a \text{sinc}(f - f_r) e^{-j\Phi_2} \quad (3.5.6)$$

The signals add constructively in a certain direction and produce a beam. The signal after striking the target is reflected back and is received by the receiver.

The received signal from one element depends on the effective area  $A_r$  and radar cross-section  $\sigma$ . The received signal is then amplified by the low noise amplifier LNA, assuming the same gain  $A_p$  as for the high power amplifier HPA. A phase shifter removes the shift that was added during transmission by adding an inverse phase.

The shape of the received spectrum is essentially intact but in practice a varying amount of noise is added.

The TR module is the most critical and expensive part of a phased array systems. The development of low cost TR modules is a very active area of research [21]. The cost is reduced by monolithic microwave integrated circuits (MMICs) but this technology is still expensive [8,20].

## Chapter four: Simulation results and analysis

### 4.1. Single element side-feed patch antenna

Figure 4.1 shows the antenna designed in chapter 3.

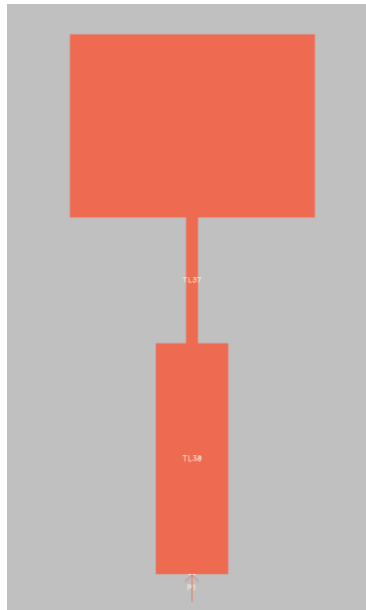


Figure 4.1: Single element side-feed patch antenna designed in ADS Momentum.

An important antenna parameter is the reflection coefficient since it also relates to the resonant frequency. The S-parameter  $S_{11}$  should have a strong dip at the resonant frequency since this corresponds to minimum reflected power. The return loss should lie below -10 dB (10% reflected power).

Figure 4.2. shows that the antenna resonates at 9 GHz with  $S_{11}$  down to almost -15 dB which is well below -10 dB.

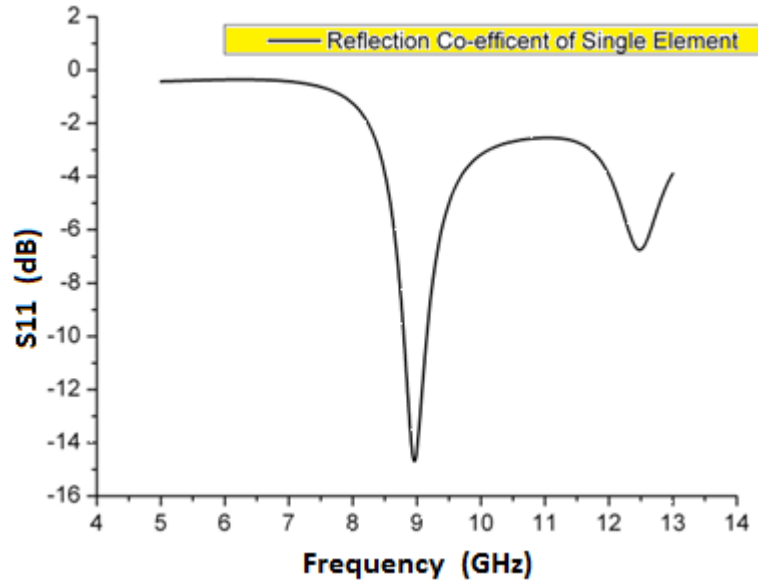


Figure 4.2: The  $S_{11}$  parameter of a single side-feed patch antenna obtained with ADS.

#### 4.1.1. Radiation pattern and gain

The radiation pattern shows the angular distribution of radiation and provides the half power beam width [2]. The microstrip patch generally has a wide beam and low gain. The radiation pattern of a single side-feed patch is shown in Figure 4.3.

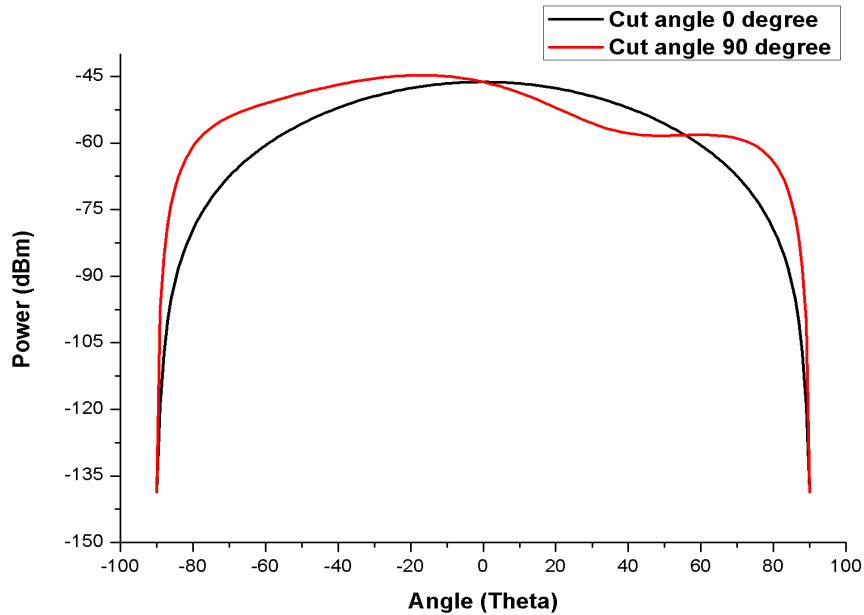


Figure 4.3: Radiation pattern of single side-feed patch antenna obtained with ADS.

The main parameters which affect the radiation pattern are the width of the patch and the height of the substrate. It can be seen from the figure that the radiation pattern cuts ( $\varphi=0^\circ$  and  $\varphi=90^\circ$ ) differ so unfortunately the antenna diagram is not symmetrical.

The gain of the single side-feed patch is shown in Figure 4.4.

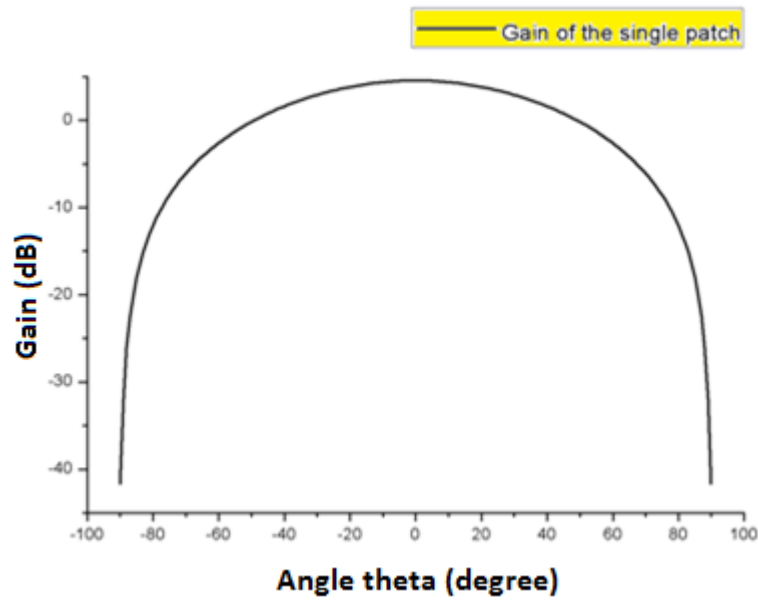


Figure 4.4: The gain of the single side-feed patch antenna obtained with ADS.

The simulated gain of the antenna is almost 2 dB at ( $\theta = 0^\circ$ ). The graph shows that the directivity is low. This type of radiation pattern suits some telecommunication applications but is not adapted to radar.

#### 4.1.2. 3D Radiation pattern

Figure 4.5 shows a three-dimensional top view ( $\theta = 0^\circ$ ) of the directivity of the single side-feed square patch antenna. The directivity is low for a single patch and the antenna radiates almost isotropically.

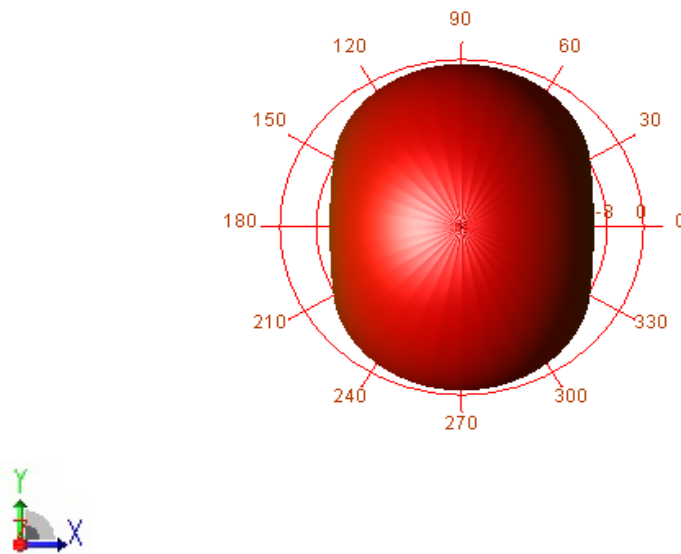


Figure 4.5: A 3D graph of the far field radiation of a single square patch antenna.

## 4.2. Simulation of a 1D phased array antenna

The linear or 1D antenna array was designed with four elements and a  $\lambda/2$  spacing as shown in Figure 4.6.

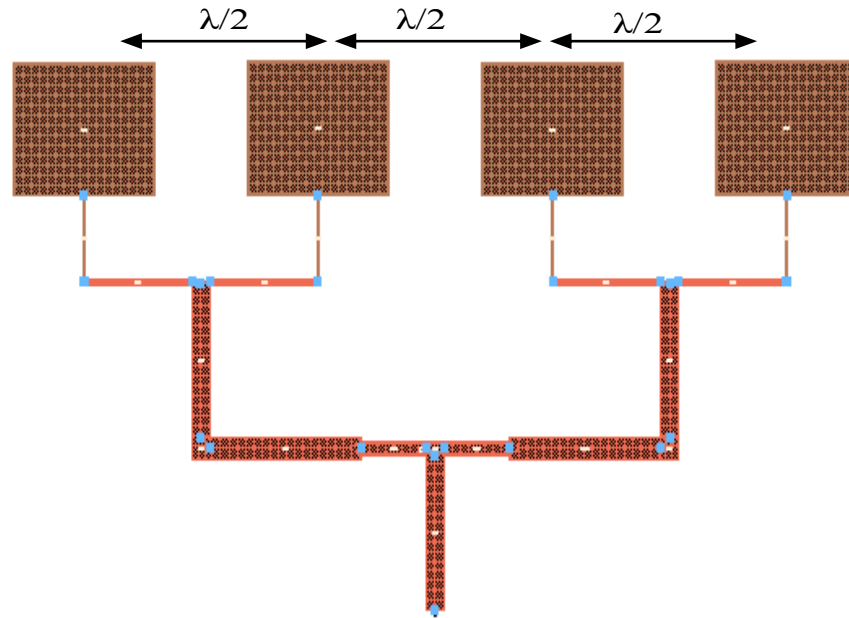


Figure 4.6: 1D phased array patch antenna designed in ADS Momentum.

### 4.2.1. Radiation pattern and gain

Figure 4.7 shows the radiation pattern of a 1D array along the x-axis ( $\varphi = 0^\circ$ ).

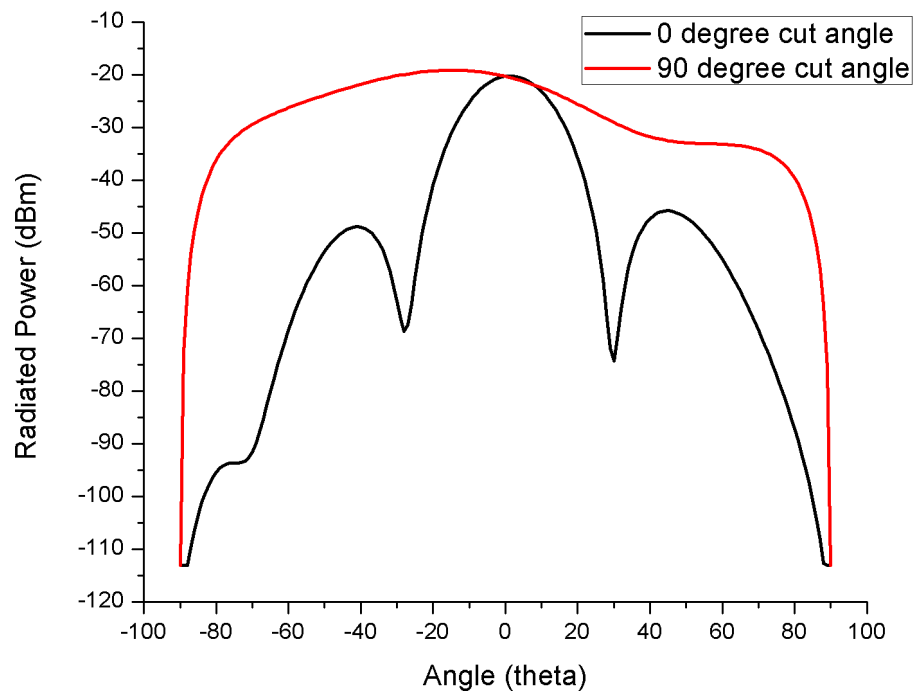


Figure 4.7: Radiation pattern of a 1D phased array antenna obtained with ADS.



It appears that the array is more directive than the single patch in the broad side cut. The  $90^\circ$  cut shows almost the same directivity as for the single element. The expected increase in gain is shown in Figure 4.8.

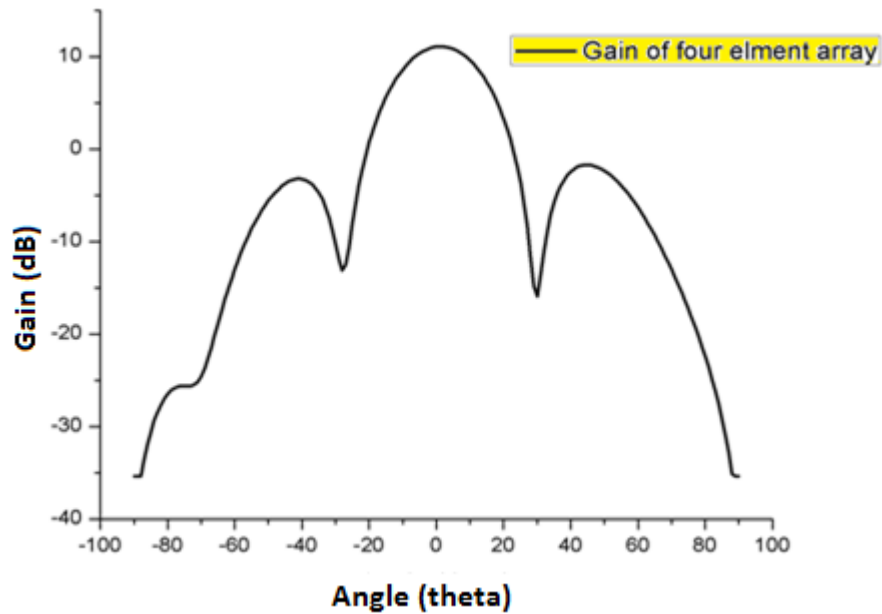


Figure 4.8: Gain of a 1D phased array antenna obtained with ADS.

Comparing the gain of the single element and the array at  $\theta = 0^\circ$  one has 2 dB and 10 dB, respectively. The improvement is 8 dB or 2 dB per element.

#### 4.2.2. 3D Radiation pattern

A 3D top view ( $\theta = 0^\circ$ ) pattern for a 1D phased array antenna is shown in Figure 4.9.

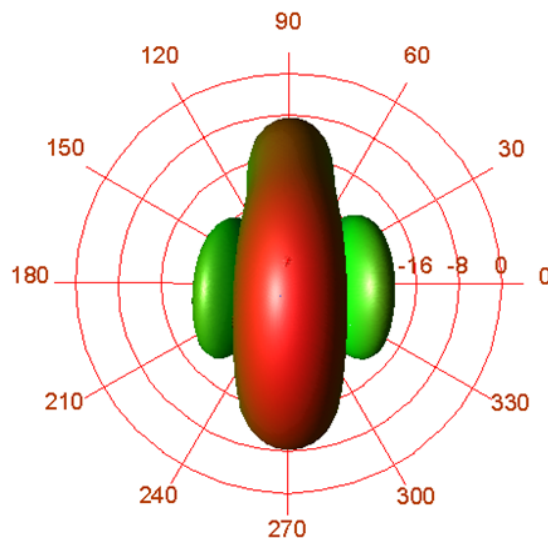


Figure 4.9: A 3D radiation pattern of a 1D phased array antenna.

Figure 4.9 shows that there is a symmetry with respect to the array axis that corresponds to a rotation of the zero-degree cut in Figure 4.7. The directivity is fairly good in the broad-side cut. Figure 4.10 shows the magnitude of the surface current on the 1D array.

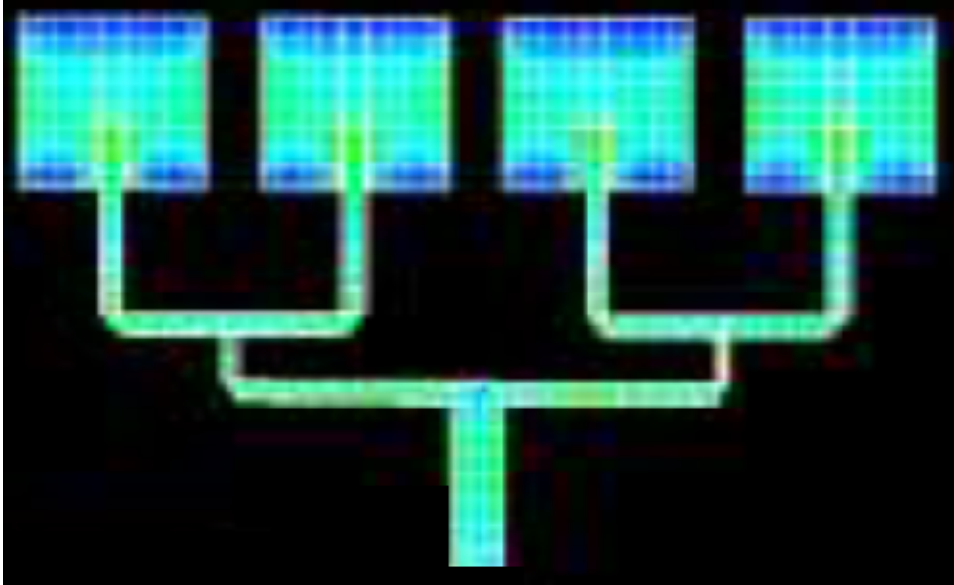


Figure 4.10: Excitation of 1D phased array antenna obtained with ADS.

### 4.3. Simulation of a 2D phased array antenna

The 2D phased array antenna is composed of sixteen elements, each with a phase shifter. The beam forming or beam steering of a 2D array is done in the same way by shifting the phase of the feed. Figure 4.11 is a top view of a 2D array in ADS Momentum.

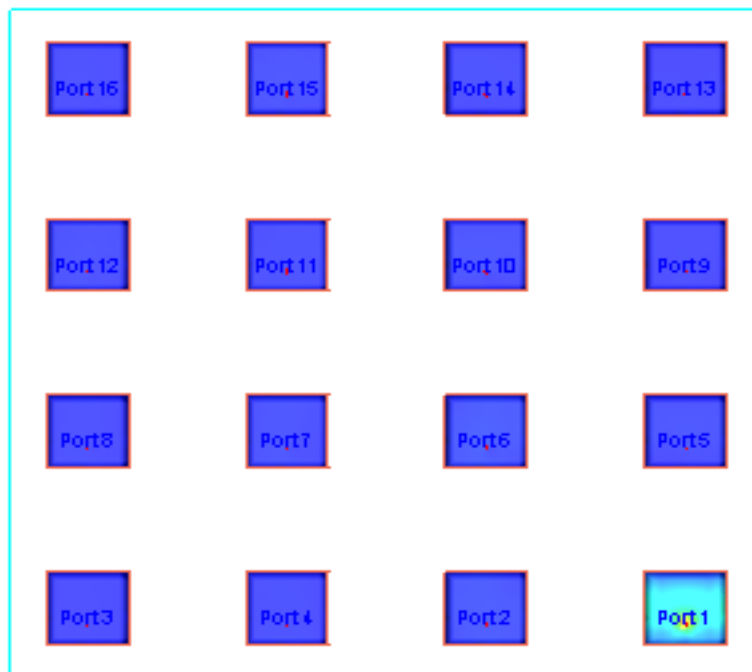


Figure 4.11: Top view of a 2D array obtained in ADS.

### 4.3.1. Directivity and gain

One of the main features of ADS Momentum is that it gives us both the 2D and 3D graphs of the gain and directivity. Figure 4.12 shows the gain and directivity of the 2D array in the  $\varphi = 0^\circ$  cut.

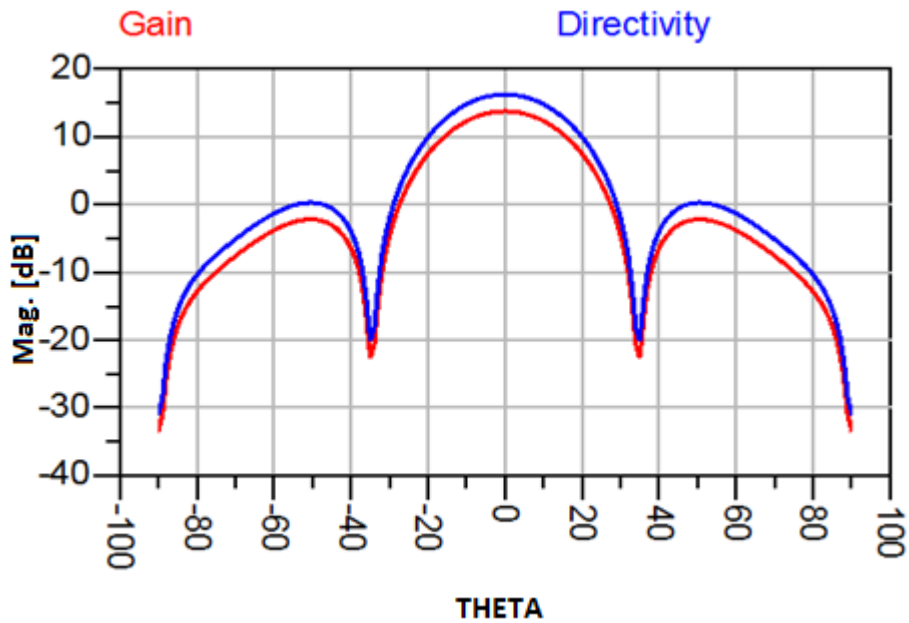


Figure 4.12: Gain and directivity of a 2D phased array antenna obtained with ADS.

As shown in the Figure 4.12, the maximum gain and directivity for the 2D array are 15 dB and 18 dB, respectively.

### 4.3.2. $S_{11}$ parameters

ADS simulation helps us in gathering information about the S-parameters of the antenna. We have used only one probe feed in our design, so only the reflection coefficient or  $S_{11}$ , for the 2D array is obtained. The simulation results are shown in Figure 4.13.

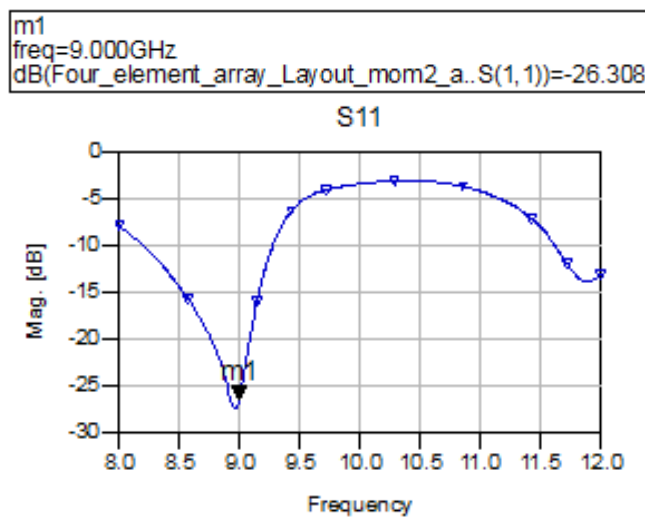


Figure 4.13: The magnitude vs frequency graph of  $S_{11}$ .

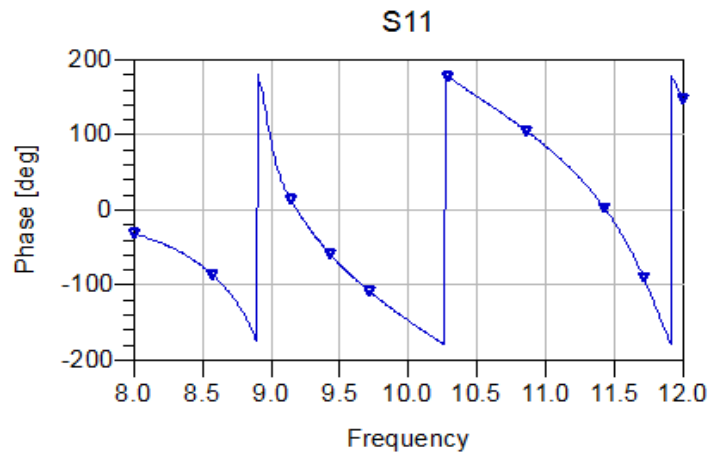


Figure 4.14: The corresponding phase of  $S_{11}$ .

```
m2
freq=9.083GHz
Four_element_array_Layout_mom2...S(1,1)=0.059 / -109.607
impedance = Z0 * (0.955 - j0.107)
```

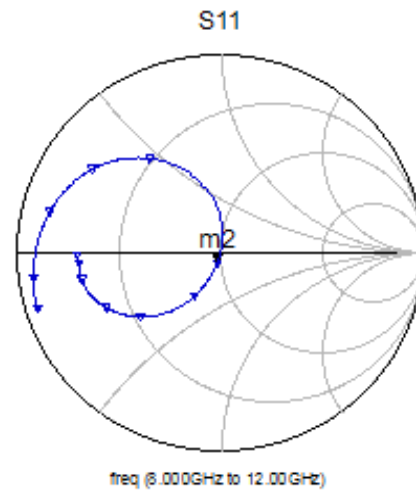


Figure 4.15:  $S_{11}$  plotted on a Smith chart for the frequency band 8-12 GHz.

From the figures it is clear that the 2D array resonates at 9 GHz with a minimum return loss of -26 dB.

### 4.3.3. Efficiency and radiated power

The efficiency of the 2D array is 82%, as shown in Figure 4.16.

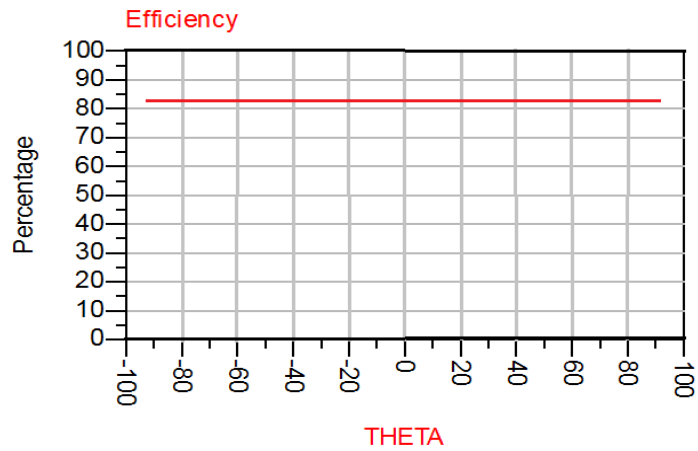


Figure 4.16: Efficiency of the 2D phased array patch antenna obtained with ADS.

The efficiency can be improved by increasing the number of elements. The power radiated by the 2D phased array is shown in Figure 4.17.

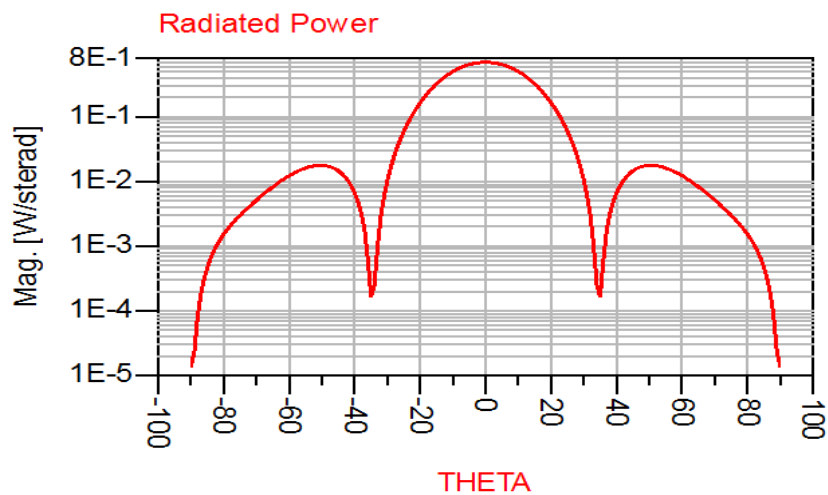


Figure 4.17: Radiated power of the 2D phased array patch antenna.

### 4.3.4. 3D Radiation pattern

Phased arrays are intended to have high directivity. Three-dimensional radiation patterns of a 2D array with sixteen elements are shown in Figure 4.18. The graph shows that the 2D array has a fairly good directivity.

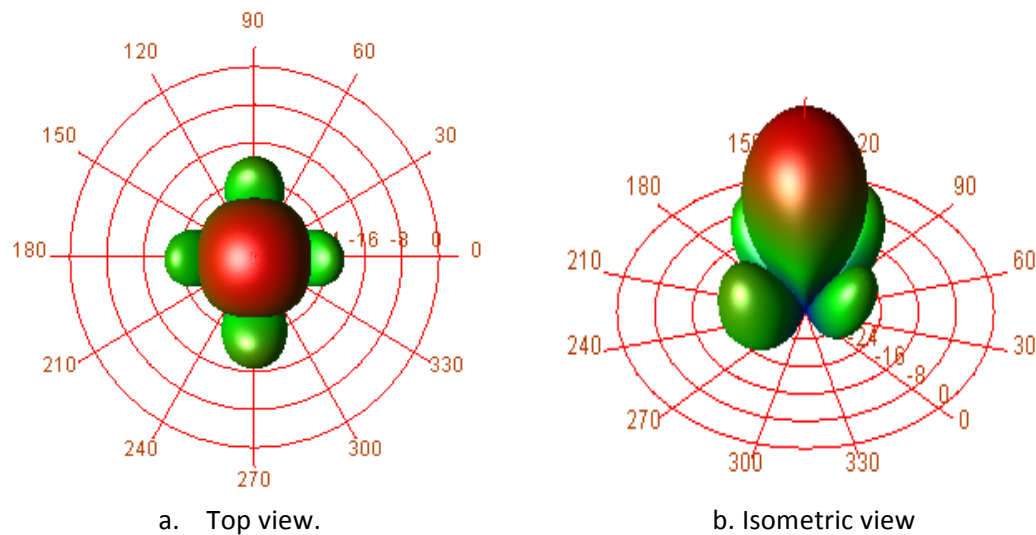


Figure 4.18: 3D directivity pattern of the 2D phased array antenna.

#### 4.4. Simulation of beam steering of a linear array

Beam scanning can be implemented with different techniques using ferrite shifters, switched line phase shifters or digital phase-shifting integrated circuits. A block diagram for beam steering is shown in Figure 4.19.

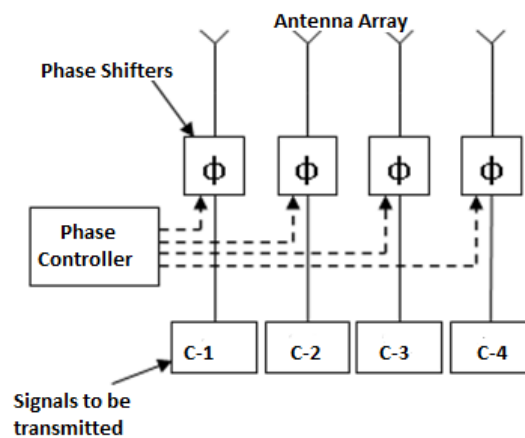


Figure 4.19: Block diagram for beam steering.

Beam steering is achieved by sending signals to each antenna element with a relative phase generated in ADS Momentum. ADS has a build-in feature for this. With no phase difference between the antenna elements one obtains the broadside radiation shown in Figure 4.20. In order to tilt the beam  $10^\circ$  to the right, a phase difference of  $31.26^\circ$  is applied to the elements. The phase of each element is shown in Table 4.1. The radiation pattern along the steering axis is shown in Figure 4.20.

Table 4.1: Relative phase of the elements in degrees.

C0	C1	C2	C3	C4
0	-31.26	-62.52	-93.78	-125.04

Figure 4.20 shows how the beam can be steered to the right/left by applying phase shifts to the elements.

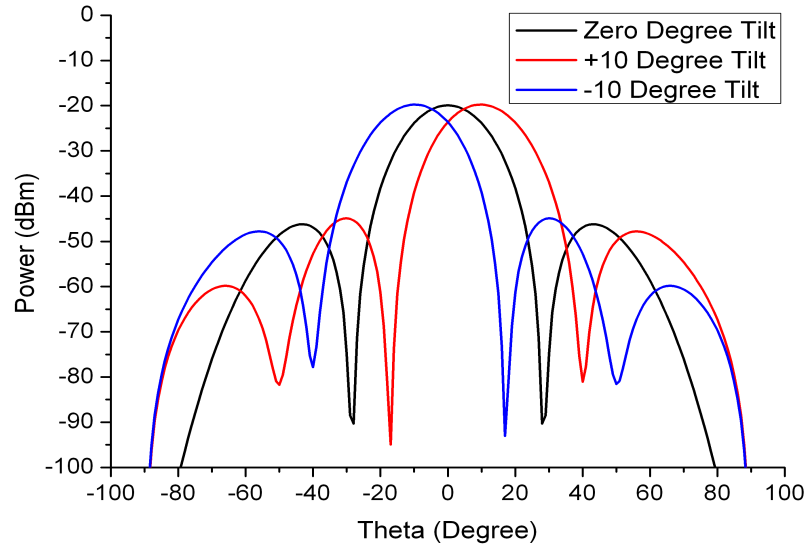


Figure 4.20: Simulation of linear array beam steering.

Figure 4.20 shows how the main beam can be tilted by means of a linear phase variation on the elements. The maximum steering angle depends on two things: the spacing between the antenna elements and the radiation pattern of the individual elements.

#### 4.5. Simulation of beam steering of a 2D array

The 2D antenna array of sixteen elements (4x4) has  $\lambda/2$  spacing between adjacent elements. In order to steer the beam in a particular direction, the relative phase difference is calculated. The antenna elements are numbered from 1 to 16 starting from the bottom left. Beam steering involves both angles. In order to steer the main beam for 3  $\theta$  values. The phase shifts are applied to the columns of the array at  $\varphi = 0^\circ$  cut. In the same way, the  $\varphi = 90^\circ$  cut is steered by means of the rows. The general case involves both columns and rows. Figure 4.21 shows steering in the  $\theta = +20^\circ$  at  $\varphi = +5^\circ$  cut and  $\theta = -20^\circ$  at  $\varphi = -5^\circ$  cut for the 2D array.

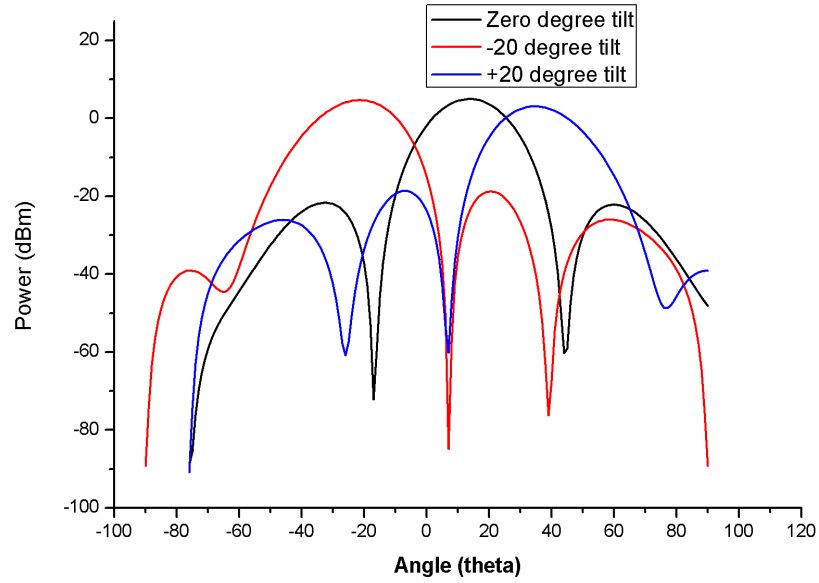


Figure 4.21: Simulation of beam steering of a 2D array.

## 4.6. The RF front end

The RF front-end is simulated in ADS Momentum. The transmitted pulses in the time and frequency domain are shown in Figure 4.22 and 4.23, respectively.

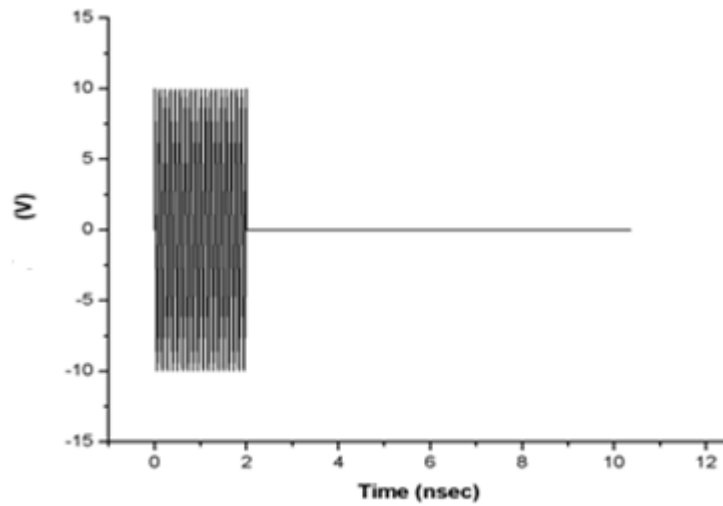


Figure 4.22: Transmitted pulse, time domain.

In the frequency domain, the transmitted RF pulse has a sinc shape centered on the carrier. This is shown in Figure 4.23 for a carrier at 9 GHz. The width of the pulse in the time domain relates inversely to the bandwidth in the frequency domain. Therefore, the wider the pulse, the narrower the bandwidth relating to the sinc. If the ON time is  $2\tau$  the first null of the sinc is  $1/\tau$ .



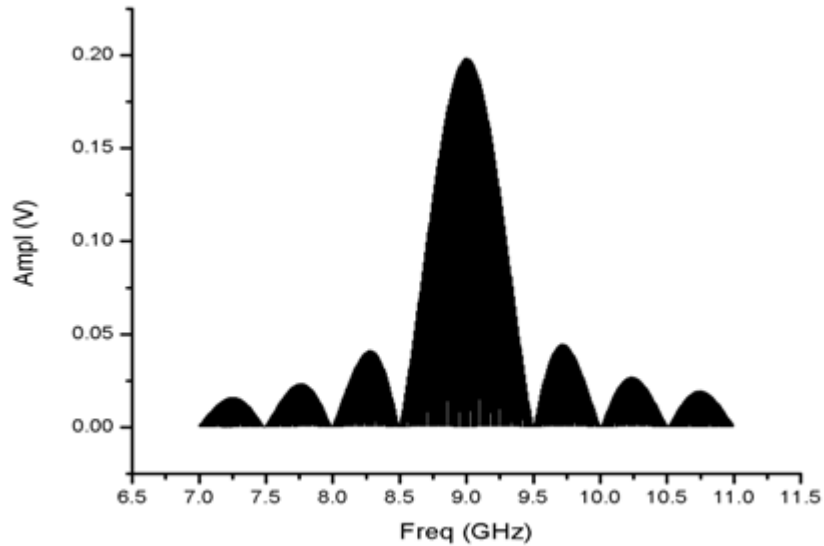


Figure 4.23: The amplitude of the transmitted pulse in the frequency domain.

A pulse width  $2\tau = 2$  ns corresponds to 1 GHz and this appears in Figure 4.23 in the form of nulls at 8.5 and 9.5 GHz.

The power divider network was designed with lumped components. A division into 16 channels gives a damping of 12 dB. The channels are fed into the high gain block of the TR module. A gain of 20 dB is used.

After leaving the TR module, the signal is transmitted and reflected back by the target. The signal strength depends on the antenna array, distance and the cross-section of the target. The reflected signal in time and frequency domain is shown in Figures 4.24 and 4.25, respectively.

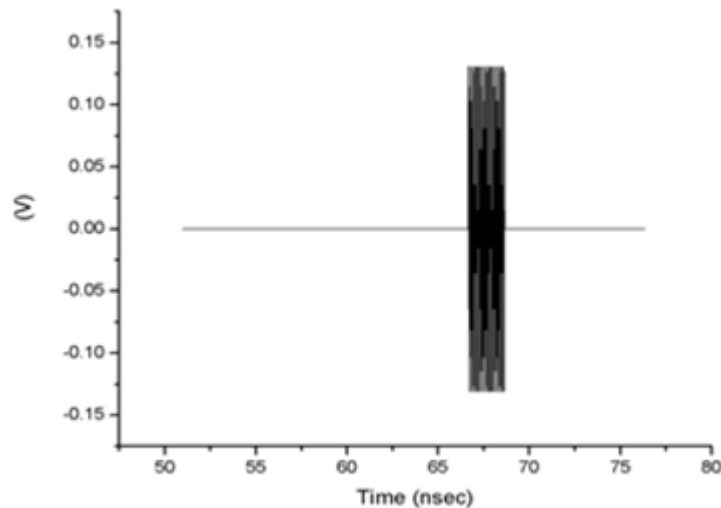


Figure 4.24: Reflected signal, time domain.

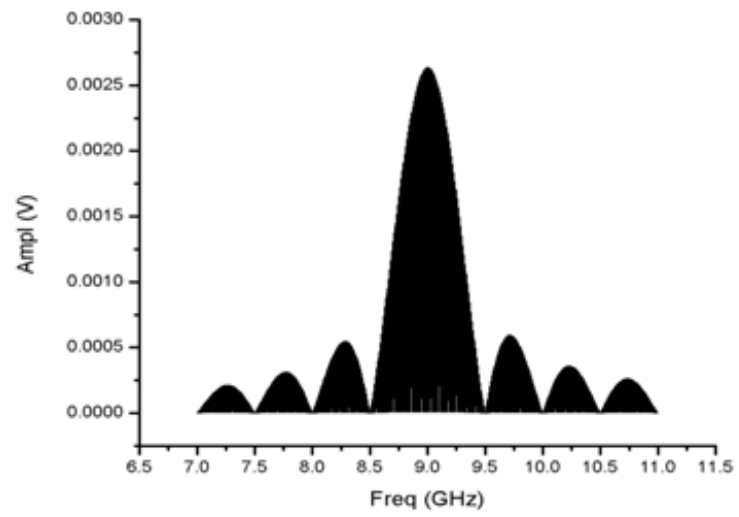


Figure 4.25: The amplitude of the reflected signal in frequency domain.

## Chapter five: Conclusion

### 5.1. Conclusion

The objective of this thesis was to design and simulate one and two dimensional phased array antennas for radar applications and to demonstrate the concept of beam steering. The control mechanism of beam steering along with the simulation of the RF front end of a phased array radar was also studied.

Four element array antennas were designed using half wavelength spacing between the elements. Beam steering was accurately simulated and the main beam was tilted in the desired direction. 2D sixteen element phased array antennas were designed with half wavelength spacing between the elements, and the main beam was steered in two directions. The RF front end of the phased array radar system was simulated.

From the simulations and the results, it was concluded that the radiation pattern of the 1D and 2D phased array patch antennas can be improved further by increasing the number of antenna elements. Moreover, it was also demonstrated that the main beam can be steered over a limited angular interval.

### 5.2. Future work

Some suggestions for future work are:

- Adding the capability of detecting and locking on to the target. This requires movement of the beam along with the target to track its trajectory.
- Extension of the model so that more than one target can be detected using multiple beams.
- Simulation of the signal processing part of the phased array radar system.
- Implementation of the modeled system at the component level, i.e. modeling of the T/R in MMIC for example.
- Adding realistic noise in the free space channel and analyzing the effect on the signal.
- Adding the direction of arrival estimation and estimation of the difference between the direction of the transmitted and received signal.

## References

- [1] D. H. Temme, A. J. Fenn, W. P. Delaney and W. E. Courtney, "The development of phased array radar technology," *Lincoln Laboratory Journal*, vol. no. 12, pp. 321-340, 2000.
- [2] C. A. Balanis, *Antenna theory*, 3rd edition, John Wiley, New York, 2005.
- [3] M.I. Skolnik, *Introduction to radar systems*, 3rd Edition, McGraw-Hill, Singapore, 1980.
- [4] R. C. Hansen, *Phased array antennas*, 1st Edition, John Wiley, New York, 1998.
- [5] A. A. Qureshi, M. U. Afzal and T. Taqueer, "Performance analysis of FR-4 substrate for high frequency microstrip antennas," *IEEE Microwave Conference Proceedings (CJMW)* , pp. 1-4, China-Japan Joint, 2011.
- [6] M. D. C. Moles, *Advances in phased array ultrasonic technology applications*, 3rd edition, Olympus NDT Series, USA, July, 2007.
- [7] A. Komijani, "Microwave Integrated phased-array transmitter in silicon," Ph. D. dissertation, California Institute of Technology, Pasadena, California, 2006.
- [8] EMS Technology Technical Staff, *Passive phased arrays for radar antennas*, Space and Technology, Atlanta, Northcross, GA, EMS Technology Inc, pp. 1-10, 2005.
- [9] N. Tucker, "An Introduction to phased array design," Active France, Technical Report no. 09:003, pp. 1-46, Apr, 2011.
- [10] A. Wessling, "Radar target modelling based on RCS measurements," M.S. Thesis, Linköping Institute of Technology, Linköping , SWE, 2002.
- [11] P. J. Oleski, S. S. Bharj, R. W. Patton and M. Thaduri, "Transmit receive module for space ground link subsystem (SGLS) and unified S-band (USB) satellite telemetry, tracking and commanding (TT and C), and communications," *IEEE Military Communications Conference, MILCOM*, pp. 880-885, vol. no. 2, 2004.
- [12] Y. Mancuso, P. Gremillet and P. Lacomme, "T/R- modules technological and technical trends for phased array antennas," *IEEE Microwave Symposium Digest*, MTT-S International, pp. 614-617, June, 2006.
- [13] D. V. Dranidis, "Shipboard phased array radars," *Waypoint Magazine*, Feb, 2003.
- [14] L. A. Wan and A. M. Madni, "Techniques in radar target modeling," *IEEE Aerospace Applications Conference, 1988. Digest*, pp. 501-518, Feb, 1988.
- [15] C. Pyo, Y. H. Cho, J. Choi and J. Chai, "High gain and broadband microstrip patch antenna using a superstrate layer," *IEEE AP Society International Symposium* , vol. no. 2, pp. 292-295, June, 2003.

- [16] G. Ahmed, "Design, optimization and development of X-band microstrip patch antenna array for high gain, low sidelobes and impedance matching," *IEEE Trans. ICEE Second International Conference on Electrical Engineering*, pp. 1-6, Mar, 2008.
- [17] P. Soontornpipit, C. M. Furse, and Y. C. Chung, "Design of implantable microstrip antenna for communication with medical implants," *IEEE MTT*, vol. no. 52, pp. 1944–1951, 2004.
- [18] I. F. Anitzine, J. A. R. Argota and B. A. Perez, "Matching of microstrip patch array antennas with reflectors," *IEEE Trans. Antennas and Propagation (EuCAP), Proceedings of the Fourth European Conference*, pp. 1-4, April, 2010.
- [19] J. Huang, "The finite ground plane effect on the microstrip antenna radiation patterns," *IEEE AP*, vol. no. 31, pp. 649-653, July, 1983.
- [20] H. J. Visser, *Array and phased array antenna basics*, 1<sup>st</sup> Edition, John Wiley, West Sussex, 2005.
- [21] P. V. D. Westhuizen and D. G. V. D. Marwe, "Design of a T/R module for a phased array radar," *IEEE Trans. 4<sup>th</sup> AFRICON*, vol. no. 2, pp. 745-748, Sep, 1996.



# **Linnæus University**

School of Computer Science, Physics and Mathematics

SE-391 82 Kalmar / SE-351 95 Växjö

Tel +46 (0)772-28 80 00

[dfm@lnu.se](mailto:dfm@lnu.se)

[Lnu.se/dfm](http://Lnu.se/dfm)